Formation of an Intracontinental Orogen Above the Permo-Triassic Mantle Convection Cell in the Paleo-Tethys Tectonic Realm due to Far-Field Stress Derived From Continental Margins

Lei Zhao[1]*, Mingguo Zhai[1] and Xiwen Zhou[2]

[1]State Key Laboratory of Lithospheric Evolution, Institute of Geology and Geophysics, Chinese Academy of Science, Beijing, China, [2]Institute of Geology, Chinese Academy of Geological Sciences, Beijing, China

The identification of intraplate orogens seemingly poses challenges to the plate tectonic theory. Delineating the formation processes of intraplate orogens can provide clues for the better understandings of the above issue. Although still controversial, the Indosinian (Permo-Triassic) orogeny in the South China Block (SCB) is potentially a good example of intracontinental orogen. In this paper, we carry out studies on the Indosinian high-grade rocks in the northeastern Cathaysia Block of the SCB, hoping to cast light on the features and formation processes of intraplate orogenic belts. These rocks exhibit HP/HT granulite facies mineral assemblages and reaction textures imply that they witnessed eclogite-facies metamorphism. Their clockwise P-T trajectories with isothermal decompression stages suggest significant crustal thickening followed by quick orogenic collapse. Immobile whole-rock trace elements indicate basaltic protoliths features, resembling E-MORB and OIB, respectively. SIMS zircon U-Pb age dating confirms Indosinian metamorphic ages of ~248 Ma and a protolith age of ~953 Ma. The mantle-like O isotopic compositions of the Neoproterozoic magmatic zircon cores further attest that they were primarily mantle derived rocks. The whole-rock Sm-Nd isotopic compositions show more enriched features because of metamorphic alteration, while zircon Lu-Hf isotopic results show primitive characteristics with Neoproterozoic model ages. These features suggest that the high-grade mafic rocks, as well as the metamorphosed early Precambrian metasedimentary rocks hosting them, are all continental crust components and juvenile oceanic crust components featuring plate margins are absent during the SCB Indosinian orogeny. Characteristics of these high-grade rocks and their spatial occurrences are both consistent with the proposal of an intracontinental orogen. After summarizations and comparisons of the Indosinian plate margin activities around the SCB, we suggest that this northeast-southwest trending orogenic belt is geometrically consistent with two mantle convection cells, with one conveying the SCB northward to collide with the North China Craton, and the other conveying the Paleo-Pacific plate northwestwards to form an active continental margin along the southeast SCB. The driving

mechanism of the formation of the SCB Indosinian intracontinental orogenic belt could have broad implications for other intraplate orogens around the world.

INTRODUCTION

The identification of intraplate orogenic belts in different parts of the world posed a challenge to the theory of plate tectonics because according to the theory, compressive stresses concentrate at plate margins where different plates interact while the interior regions of plates are rigid and hard to deform. The intraplate orogens refer to those formed at large distances from active plate boundaries, with driving forces from both plate-boundary and intraplate stress sources (Raimondo et al., 2014). Several examples of intraplate orogens have been proposed and studied in different parts of the world, like central Asia and central Australia (Sandiford and Hand, 1998; Yin et al., 1998; Hand and Sandiford, 1999; Sandiford et al., 2001). Intraplate orogens might also occur in oceanic plates, but examples are difficult to find due to their inaccessibility. Albeit these good examples, the occurrences of large-scale compressional intraplate orogens are relatively rare, especially in the Phanerozoic during which modern plate tectonics dominate geological processes. The Permo-Triassic deformation in the South China Block has long been termed as the Indosinian Movement in the Chinese literature (Cui and Li, 1983; Huang, 1984; Ren, 1984; Wang et al., 2013a; Zhang et al., 2013), and is potentially another good example of intraplate orogenic belt, although different opinions exist (Hsü et al., 1988; Gupta et al., 1989; Rowley et al., 1989; Hsü et al., 1990; Faure et al., 2018; Lin et al., 2018; Shu et al., 2018).
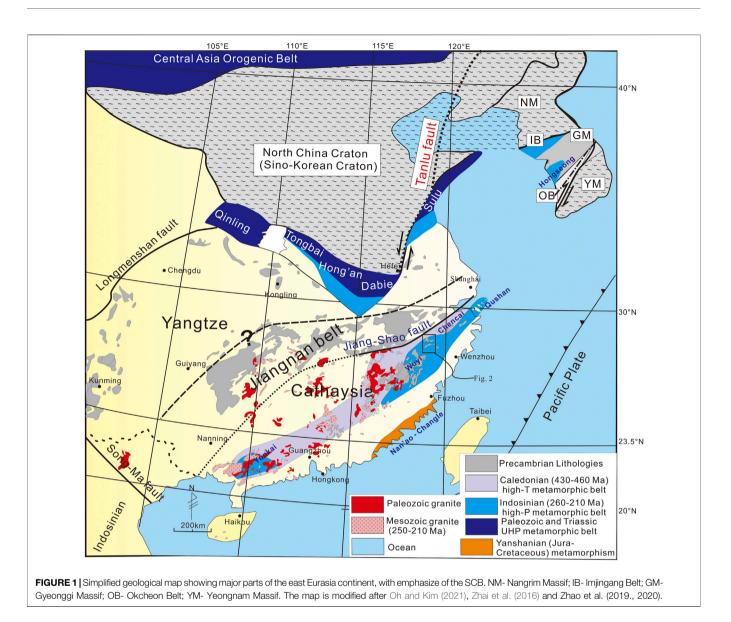
Researchers who proposed the intracontinental setting for the SCB Indosinian orogen believe that the SCB gained and retained its integrity ever since Neoproterozoic, and besides, they found that this orogeny caused mainly thin-skinned tectonics involving reactivation of only ancient continental components (Chen et al., 1991; Li, 1998; Li and Li, 2007; Shu et al., 2008b; Li S. et al., 2012; Shu, 2012; Faure et al., 2016a; Faure et al., 2016b). On the contrary, other researchers suggested a plate margin setting for this orogenic belt (Guo et al., 1984; Hsü et al., 1988; Zhao et al., 1996; Yin et al., 1999; Lin et al., 2018). Hsü et al. (1988) proposed that the SCB Indosinian orogeny was the result of continental collisions between the Yangtze and Cathaysia Blocks, based mainly on the inference that the Banxi Group (mainly in the Jiangnan belt) is a tectonic mélange that accommodated significant crustal shortening through long-distance thrusting. However, other tectonic observations, as well as isotopic ages which show that the Banxi Group represents the Precambrian basement of the SCB, contradict this continental collisional model (Gupta et al., 1989; Rowley et al., 1989; Chen et al., 1991). Due to the lack of high-grade metamorphism, tectonic models like multiple-terrane accretion and soft-collision have also been proposed for the SCB Indosinian orogeny (Guo et al., 1984; Yin et al., 1999). Lin et al. (2018) suggested an Appalachian-style multi-terrane Wilson cycle model for the SCB, in which they

argued that the Indosinian orogen was the result of continental collisions between the East and West Cathaysia Blocks. Even though criticisms exist (Faure et al., 2018; Shu et al., 2018), the Triassic high-grade metamorphic rocks, including retrograded eclogites and granulites in the northern Wuyi terrane of the Cathaysia Block, as well as their clockwise P-T trajectories, seem reminiscent those of continental margin orogenic belts (Zhao L. et al., 2017; Xia et al., 2021).

Continental crust, no matter intraplate or proximal to plate margins, will experience crust shortening, thickening, uplifting and exhumation of high-grade metamorphic rocks after accommodating strain (Raimondo et al., 2014). High-grade metamorphism, therefore, can be unhelpful in discriminating intraplate and plate margin orogenic belts. The occurrences of ophiolitic mélange, however, can directly demarcate plate boundaries. Besides, protolith features of high-grade metamorphic rocks and the spatial distributions of orogenic high-grade metamorphic rocks can also provide clues for the discriminating of an orogenic belt. In this paper, we present new studies on the Indosinian high-grade rocks in the northern Wuyi terrane of the Cathaysia Block which represent the uplifted orogenic core components. Based on this new data and a summarization of Indosinian orogenic events around the SCB, we proposed a new interpretation of the SCB Indosinian orogeny and the related deep geodynamic processes for its formation.

GEOLOGICAL BACKGROUND

The SCB situated in the southeastern Eurasia continent is now demarcated by the Central China Orogenic belt in the north from the North China Craton and facing the Tibetan Plateau in the west, the Pacific plate in the east and south (**Figure 1**). Such a triangular region is believed to receive stress from all directions since at least Mesozoic (Li S. et al., 2012), generating the current geometry of the SCB. This continental block is normally believed to have gained its integrity since Neoproterozoic through the amalgamation of the Yangtze and Cathaysia Blocks Li et al., 2009a; Wang X.-L. et al., 2014; Wang Y. et al., 2014; (Li L. et al., 2016; Zhao G. et al., 2018; Zhao J.-H. et al., 2018; Shu et al., 2019). This continental collisional event resulted in the formation of the Jiangnan belt hosting a great amount of the Neoproterozoic sequences of the SCB (Li et al., 2009a; Wang X.-L. et al., 2014; Wang Y. et al., 2014; Li L. et al., 2016; Zhao J.-H. et al., 2018; Shu et al., 2019). Two other episodes of tectonothermal events during Phanerozoic besides the Indosinian orogeny occurred in the SCB, termed as the South China Caledonian orogeny (Paleozoic) and the Yanshanian (Jura-Cretaceous) orogeny in the Chinese literature.

The SCB Caledonian orogeny affected many of the pre-Devonian sequences of the SCB and caused the unconformity

FIGURE 1 | Simplified geological map showing major parts of the east Eurasia continent, with emphasize of the SCB. NM- Nangrim Massif; IB- Imjingang Belt; GM- Gyeonggi Massif; OB- Okcheon Belt; YM- Yeongnam Massif. The map is modified after Oh and Kim (2021), Zhai et al. (2016) and Zhao et al. (2019., 2020).

between the Devonian sequences and the pre-Devonian metamorphic crystalline basement (Chen X. et al., 2012, Chen et al., 2014; Li J. et al., 2016; Wang Y. et al., 2012, Wang et al., 2013a; Zhang et al., 2013; Shu, 2012). Lines of evidence from lithofacies and biofacies suggested that the Paleozoic orogeny was initiated in the southeastern SCB and stepwise developed toward the northwest direction (Chen X. et al., 2012; Chen et al., 2014). Paleozoic high-grade metamorphism and crustal anatexis widely occur in regions along the Jiangshan-Shaoxing (Jiang-Shao) fault (**Figure 1**, Yu et al., 2003, Yu et al., 2005; Zeng et al., 2008; Zhao et al., 2016, Zhao et al., 2019, Zhao et al., 2020), usually interpreted to be the uplifted orogenic root sequences of the South China Caledonian orogenic belt (Hsü, 1989). Geochronological studies of the Paleozoic metamorphism and anatexis constrain the duration of this event to be between ~460 Ma and 410 Ma, with most metamorphic ages from granulite-facies rocks peaking at ~450 Ma and ~430 Ma

(Yu et al., 2003, 2005; Zeng et al., 2008; Zhao et al., 2016; Zhao et al., 2019; Zhao et al., 2020). The metamorphic signatures of the SCB Yanshanian orogeny are mainly preserved along the southeastern coastal regions, represented by extensive migmatitic rocks (**Figure 1**, Liu Q. et al., 2012; Xing et al., 2010, Xing et al., 2014).

The Indosinian orogeny affected large areas of the SCB, but the related high-grade metamorphic signatures occur mainly in the Wuyi terrane of the northeastern Cathaysia Block and are sandwiched by the Caledonian and Yanshanian high-grade metamorphic regions (**Figure 1**). Earlier studies of the Wuyi terrane emphasized mainly the antiquity of the Precambrian sequences (Li, 1997; Yang and Jiang, 2019; Yu et al., 2007, Yu et al., 2009, Yu et al., 2010; Zhao et al., 2014), because they are the critical lithologies that can potentially solve the long-lasting controversy about whether the Cathaysia Block contains "Oldland" (ancient crystalline basement, Grabau, 1924; Hu and Ye, 2006; Lu, 2006; Yu et al., 2006). Besides
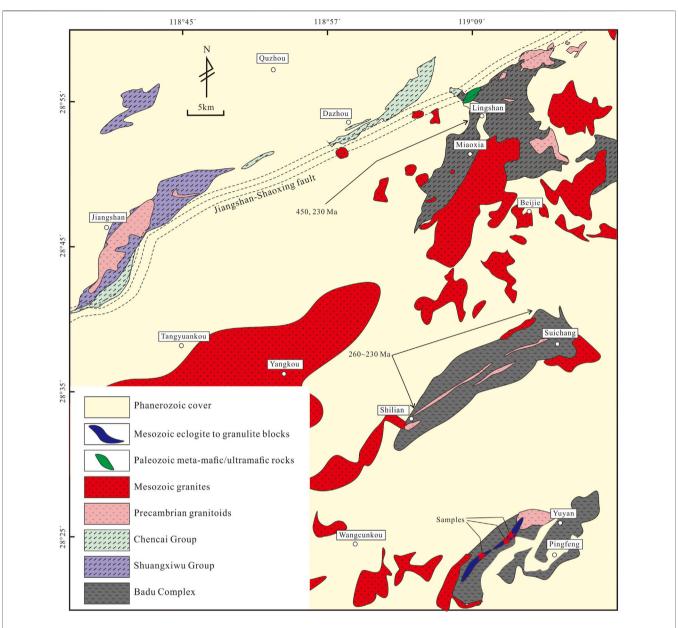
FIGURE 2 | Detailed geological map of the study area showing relations with the Jiang-Shao fault. Right to the south of the fault, both Caledonian and Indosinian metamorphism can be seen. Modified after (Zhejiang GBMR, 1980).

the early Precambrian ages (mainly ~1900–1800 Ma), the Indosinian metamorphic ages are widely identified from these lithologies in these early studies, ranging from 260 Ma to 230 Ma (Xiang et al., 2008; Yu et al., 2009, 2012; Zhao et al., 2014, 2015; Chen et al., 1998). These early Precambrian lithologies have been defined as the Badu and Mayuan complexes and were not found in other parts of the Cathaysia Block (**Figure 1**). Supracrustal sequences, as well as Paleoproterozoic granitoids of these two lithological units, also show Paleoproterozoic metamorphic alterations at ~1.85 Ga, interpreted to be related to the supercontinent Columbia (Yu et al., 2009; Xia et al., 2012; Yu et al., 2012; Zhao et al., 2014). Lin et al. (2018), as mentioned earlier,

suggested that the Indosinian metamorphic ages represent the time of a continental collisional event between the East and West Cathaysia.

The Indosinian retrograded eclogites and mafic granulites of the SCB were found to occur mainly in the Wuyi terrane and they are entrained lenticular blocks within the metamorphosed supracrustal rocks of the Badu Complex, which occur to the south of the Jiang-Shao fault (**Figure 2**, Zhao L. et al., 2017; Zhao L. et al., 2018). Rocks of this lithological unit occurring close to the fault exhibit both Paleozoic (~450 Ma) and Indosinian metamorphism (Chen et al., 2015; Zhao et al., 2015; Wang JG. et al., 2014). Rocks occurring further south, like those Paleoproterozoic supracrustal rocks and granitoids
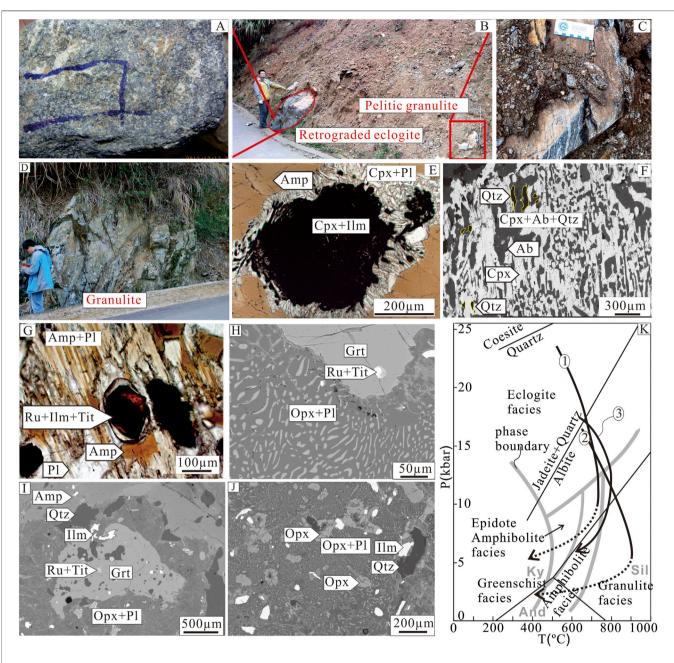
FIGURE 3 | Field photographs **(A–D)**, photomicrographs **(E–J)** showing field occurrences, representative mineral assemblages and reaction textures, and P-T trajectories of the Indosinian high-grade rocks in the Wuyi terrane of the Cathaysia Blocks. Field and micrographic photos are from Zhao L. et al. (2018) and Zhao L. et al. (2017). Numbers in **(K)**, 1 and 2 are P-T trajectories for retrograded eclogite and mafic granulite samples, respectively (from Zhao L. et al., 2017); 3 is P-T trajectory for retrograded eclogite presented by Xia et al. (2021). Mineral abbreviates, Amp, amphibole; Cpx, clinopyroxene; Pl, plagioclase; Ilm, ilmenite; Qtz, quartz; Ab, albite; Ru, rutile; Tit, titanite; Grt, garnet; Opx, orthopyroxene.

in the Suichang-Shilian area, show Indosinian high-grade metamorphism and the Caledonian overprinting is absent (Yu et al., 2012; Zhao et al., 2014). Permo-Triassic (254 Ma, 232–215 Ma) syenites and A-type granites interpreted to represent post-orogenic extensional setting have also been reported from this area within the Indosinian metamorphic belt defined in **Figure 1** (Wang Q. et al., 2005; Sun et al., 2011; Li W. et al., 2012; Sun et al., 2017).

SAMPLES

In order to get a better understanding of the protolith features as well as the driving mechanism of the Indosinian orogenic processes in the SCB, the retrograded eclogite and mafic granulite samples occurring in the Wuyi terrane of the Cathaysia Block were collected and studied in this paper, including five retrograded eclogite samples, and five mafic

granulite samples (**Supplementary Table S1**). The metamorphism of these rocks has been presented in a previous paper (Zhao L. et al., 2017). The retrograded eclogite occurs as entrained lenticular blocks within the pelitic granulites of the Badu Complex, whose sizes ranging from tens of centimeters to several meters (**Figure 3**). The long axes of the retrograded eclogite blocks are always parallel with the foliations of the hosting pelitic granulite gneiss. The mafic granulites occur either as deformed dykes or lenticular bodies with varying dimensions hosted by the pelitic granulite gneisses of the Badu Complex (**Figure 3D**).

Mineral assemblages of the retrograded eclogite samples are garnet + plagioclase ± clinopyroxene + amphibole + biotite + quartz and some accessary minerals like ilmenite, rutile, titanite and zircon (**Supplementary Table S1**; **Figures 3E–G**). Two of the retrograded eclogite samples (WY10-1, and -2) experienced stronger metamorphic retrogression whose clinopyroxene grains have been replaced by amphibole. Except for these two samples, clinopyroxene grains are present in all other samples and garnet grains in all the samples develop symplectites composed of fine-grained minerals of clinopyroxene + plagioclase, indicating isothermal decompressions during metamorphism (Zhao L. et al., 2017). Diagnostic eclogite facies mineral of omphacite is absent in all the retrograded eclogite samples, but symplectites of omphacite grains can be seen. The intergrowth of clinopyroxene and albite (**Figure 3F**) imply that they were replacement products of omphacite grains formed through retrograde decompressional metamorphism (Zhao L. et al., 2017). Another petrographic sign implying eclogite facies metamorphism is the absence of plagioclase grains in the matrix. All the observed plagioclase grains occur within the symplectites, either as intergrowths together with clinopyroxene replacing omphacite, or around garnet grains together with clinopyroxene or orthopyroxene or amphibole replacing garnet (**Figures 3E–G**). High-pressure facies minerals like rutile, intergrowth of clinopyroxene and ilmenite can also be seen (**Figures 3E,G**).

The mineral assemblages of the mafic granulite samples are garnet + plagioclase + orthopyroxene + amphibole + biotite + quartz and some accessary minerals like rutile, ilmenite, titanite and zircon (**Supplementary Table S1**). The mafic granulite samples can be further divided into two groups according to their consisting minerals. Compared with group A granulite samples, the two granulite samples in group B contain very few quartz grains and more garnet and amphibole grains. But the mineral assemblages and typical reaction textures of them are the same. The absence of plagioclase in the matrix implies that the mafic granulites might have also experienced eclogite facies metamorphism. Decompressional symplectitic textures can be observed around most garnet grains and they are mainly composed of fine-grained orthopyroxene + plagioclase, and occasionally fine-grained amphibole + plagioclase intergrowths (**Figures 3H–J**).

Previous metamorphic studies on these two kinds of rocks revealed clockwise P-T trajectories and Indosinian metamorphic ages of 251–245 Ma (**Figure 3K**, Zhao L. et al., 2017). Retrograded eclogite samples record metamorphic pressure peak conditions of 500–560°C, 23–24 kbar and these for the granulite samples are 600–720°C, >13 kbar (**Figure 3K**, Zhao L. et al., 2017). High-grade metamorphic rocks with similar metamorphic conditions and P-T trajectories have also been reported from the neighboring regions (Jiang et al., 2016; Xia et al., 2021). The metamorphic conditions of these rocks imply significant crustal thickening (doubled) based on a simple evaluation using lithostatic stresses. Therefore, there might be an orogenic plateau in this region during the Indosinian orogeny. In combination, the spatial occurrences of these Indosinian high-grade rocks define the northeast-southwest striking direction of the Indosinian orogenic belt of the Cathaysia Block, likely representing the uplifted orogenic core (**Figure 1**).

ANALYTICAL TECHNIQUES

Most of the experiments of this study were carried out at the State Key Laboratory of Lithospheric Evolution of the Institute of Geology and Geophysics, Chinese Academy of Sciences (IGGCAS), except for the zircon CL images. The X-ray fluorescence (Shimadzu XRF-1700/1500) was used for major element analyses, after fusion of the samples with lithium tetraborate. After baking the samples for 1 h under a constant temperature at 1000°C, the loss-on-ignition (LOI) was measured as the weight loss of the samples. The Chinese national standard sample GBW07101-07114 is used for corrections. The precision of the results is better than 0.2 wt%. Trace element analyses were performed using an ELEMENT ICP-MS after HNO_3 + HF digestion of about 40 mg sample powder for each specimen in a Teflon vessel. The Chinese national standard samples GSR1 (granite) and GSR3 (basalt) were used during analyses for accuracy and reproducibility. The relative standard deviation was better than 5% above the detection limits.

After crushing the samples, standard heavy-liquid and magnetic techniques were used in zircon grain separation and then the grains were handpicked under a binocular microscope. The zircon grains, together with zircon standards (see detailed descriptions below), were then cast in epoxy discs, and then were ground and polished to expose mid-sections of the grains for CL imaging, U-Pb dating, O (oxygen) and Lu-Hf isotope analyses. The internal zoning of zircons was examined using a CL detector (Garton Mono CL3+) equipped on a Quanta 200F ESEM with 2-min scanning time at conditions of 15 kV and 120 nA at the Peking University.

The zircon oxygen isotope was analyzed using the CAMECA IMS 1280 SIMS. Detailed analytical procedures were described by Li et al. (2010c). The Intensity of ^{16}O was typically no less than $1×10^9$ counts per second (cps). The instrumental mass fractionation factor (IMF) is corrected using zircon standard Penglai with a $\delta^{18}O$ (VSMOW) value of 5.3 ± 0.1‰ (2σ) (Li et al., 2010c). The standard data were collected regularly throughout the analytical session as the IMF drifted with time. The Qinghu zircon standard was measured as an unknown and yielded a standard deviation of 0.3 per mil (2σ), which is used for least uncertainty for individual analysis. Uncertainty on individual analysis is usually better than 0.2–0.3‰ (2σ).

SIMS zircon U-Pb dating was conducted using another CAMECA IMS 1280 SIMS. Detailed analytical procedures can be found in Li et al. (2010b) and Li et al. (2009b). During analysis, the O_2^- primary ion beam was accelerated at 13 kv. The ellipsoidal spot size is about $20 \times 30 \, \mu m$. Zircon standard Plešovice, with the age of 337 Ma (Sláma et al., 2008), was used to calibrate the measured Pb/U ratios. A long-term uncertainty of 1.5% (1RSD) for $^{206}Pb/^{238}U$ measurements of the Plešovice standard was propagated to the unknowns, despite that the measured $^{206}Pb/^{238}U$ error in a specific session is generally around 1% (1RSD) or less (Li et al., 2010c). The Pb isotopic compositions of each spot were corrected for common Pb using non-radiogenic ^{204}Pb. An average present-day crustal Pb composition (Stacey and Kramers, 1975) was used for common Pb assuming that the common Pb was largely due to surface contamination introduced during sample preparation. The data were processed using the ISOPLOT program (Ludwig, 2012). The analyzed standard Qinghu zircon as unknown gave a weighted mean $^{206}Pb/^{238}U$ age of 159.9 ± 1.9 Ma (MSWD = 0.87), consistent with the recommended $^{206}Pb/^{238}U$ age of 159.9 ± 0.2 Ma (2 SE) (Li et al., 2009b).

Zircon Hf isotope analyses were carried out using a Neptune MC-ICPMS. The spot size of 40 or 60 μm was applied during ablation with a 193 nm laser, using a repetition rate of 10 Hz in most cases. Detailed descriptions of the instrument and analytical procedures are similar to those in Wu et al. (2006). Two zircon standards, GJ and Mud Tank, whose Hf isotope compositions have been proven to be quite uniform (Woodhead and Hergt, 2005; Zeh et al., 2007; Xie et al., 2008), were used to monitor the stability of the instrument during analyses. In the analytical sessions reported here, the weighted $^{176}Hf/^{177}Hf$ (c) value of GJ is 0.2820035 ± 0.0000041, and the weighted $^{176}Hf/^{177}Hf$ (c) of the Mud tank is 0.282495 ± 0.000005, which, after considering the analytical errors, are consistent with the values recommended previously (Woodhead and Hergt, 2005; Zeh et al., 2007; Xie et al., 2008). Model ages ($T_{DM}(Hf)$) and $\varepsilon_{Hf}(t)$ of zircon grains were calculated based on depleted mantle and chondrite sources. The value of $^{176}Hf/^{177}Hf$ and $^{176}Lu/^{177}Hf$ of modeled depleted mantle are 0.28325 and 0.0384 (Griffin et al., 2002) and for chondrite 0.282772 and 0.0332, respectively (Blichert Toft and Albarede, 1997). The decay constant of ^{176}Lu adopted in this paper is 1.867 $\times 10^{-11}$ per year (Söderlund et al., 2004).

Detailed descriptions of instruments involved and analytical procedures for whole-rock Sm-Nd isotopic analyses are presented in Li C.-f. et al. (2011)), Li et al. (2011 C.-F.) and Yang et al. (2010). Very fine-grained whole-rock powders for Nd isotopic analyses were dissolved in Savillex Teflon screw-top capsules after being spiked with mixed ^{149}Sm-^{150}Nd tracers before HF + HNO_3+$HClO_4$ dissolution. For Sm and Nd separation, we used the classical two-step ion-exchange chromatographic method. The samples were then measured using a Finnigan MAT262 multi-collector thermal ionization mass spectrometer. The blank during the whole procedure was lower than 100 pg. The isotopic ratios were corrected for mass fractionation by normalizing to $^{146}Nd/^{144}Nd = 0.7219$. The international standard, JNdi-1, was employed to evaluate instrument stability during the period of data collection. The measured

values for JNdi-1 were $^{143}Nd/^{144}Nd = 0.512104 \pm 0.000007$ (*n* = 3, MSWD = 0.38). USGS reference material BCR-2 was measured to monitor the accuracy of the analytical procedure, and yielded the following result: $^{143}Nd/^{144}Nd = 0.512624 \pm 0.000012$, which is consistent with the suggested value of BCR-2 yielded by TIMS and MC-ICP-MS techniques (Yang et al., 2010; Li C.-f. et al., 2011; Li C.-F. et al., 2011).

ANALYTICAL RESULTS

All the ten samples in **Supplementary Table S1** were analyzed for whole-rock chemical compositions, while six of them were analyzed for whole-rock Sm-Nd isotopic compositions, and only two representative retrograded eclogite samples (WY1215 and WY1216) and one granulite sample (WY11) were chosen for zircon U-Pb, O and Lu-Hf isotopic analyses.
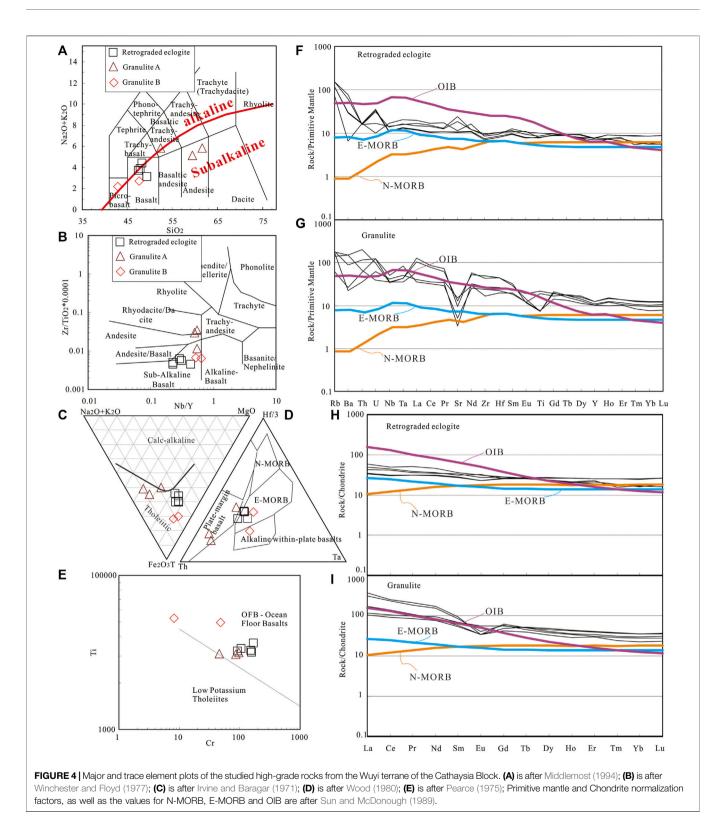
Whole-Rock Geochemistry

Major and trace element concentrations of the analyzed samples are presented in **Supplementary Table S2** and **Figure 4**. The retrograded eclogite samples have SiO_2, Al_2O_3 contents of 47.52–49.35 wt%, 12.25–15.13 wt%, respectively. They plot within the basalt field and sub-alkaline basalt field in TAS and Nb/Y *vs.* Zr/TiO_2*0.0001 diagrams (**Figures 4A,B**). In other diagrams, the retrograded eclogite samples show tholeiitic and E-MORB compositions (**Figures 4C,D**), and they belong to ocean floor basalts (**Figure 4E**). The spider diagram and chondrite normalized REE distribution patterns of the retrograded eclogite samples exhibit similarities with E-MORB (**Figures 4F,H**).

The mafic granulite samples exhibit large variations in major elements, and they plot in picro-basalt—basalt—andesite fields (**Figure 4A**). Group A granulite samples have higher SiO_2, Al_2O_3, and lower MgO, Fe_2O_3T contents compared with samples of Group B, consistent with the above observations that the ferromagnesian mineral contents of Group A granulite samples are lower than those of Group B. In the Nb/Y *vs.* Zr/TiO_2*0.0001 diagram, these samples plot within the sub-alkaline—andesite—dacite fields (**Figure 4B**). The mafic granulite samples are also tholeiitic and belong to ocean floor basalts as shown in discrimination diagrams (**Figures 4C–E**). The spider diagram and chondrite normalized REE distribution patterns of the mafic granulite samples exhibit similarities with OIB (**Figures 4F,H**).
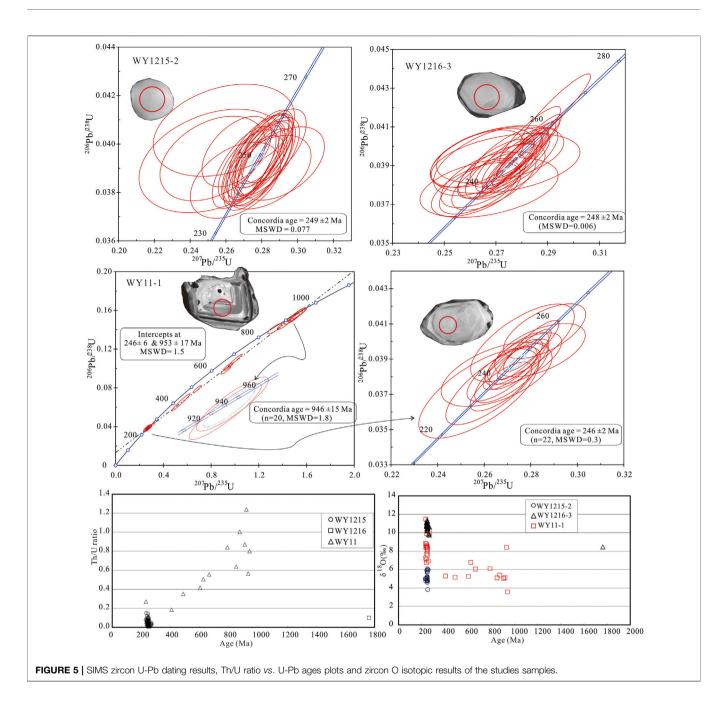
Zircon U-Pb Age Dating

The three high-grade rocks have all been dated in a previous study, using the LA-ICPMS zircon U-Pb method, which gave metamorphic ages of 245–251 Ma, and also a protolith age of 997 ± 27 Ma for the mafic granulite sample (Zhao L. et al., 2017). In this study, zircons of the two retrograded eclogite samples exhibit similar appearance and internal structures (**Figure 5**). The zircon grains are rounded, small ellipsoidal and are multi-faceted. They are unzoned or show fir-tree zoning patterns, implying metamorphic origins (Vavra, 1990). These two retrograded eclogite samples give uniform apparent $^{206}Pb/^{238}U$ ages with

FIGURE 4 | Major and trace element plots of the studied high-grade rocks from the Wuyi terrane of the Cathaysia Block. **(A)** is after Middlemost (1994); **(B)** is after Winchester and Floyd (1977); **(C)** is after Irvine and Baragar (1971); **(D)** is after Wood (1980); **(E)** is after Pearce (1975); Primitive mantle and Chondrite normalization factors, as well as the values for N-MORB, E-MORB and OIB are after Sun and McDonough (1989).

low Th/U ratios and they constrain metamorphic ages of 248–249 Ma (**Figure 5**; **Supplementary Table S3**). Some of the zircon grains of the mafic granulite sample show core-rim structures with cores exhibiting oscillatory zoning while rims

without zoning or showing fir-tree zoning (**Figure 5**). The zircon cores that do not show core-rim structures are mostly unzoned or show fir-tree zoning or sector zoning. The analytical results define a Discordia with an upper intercept age at 953 ± 17 Ma and a

FIGURE 5 | SIMS zircon U-Pb dating results, Th/U ratio *vs.* U-Pb ages plots and zircon O isotopic results of the studies samples.
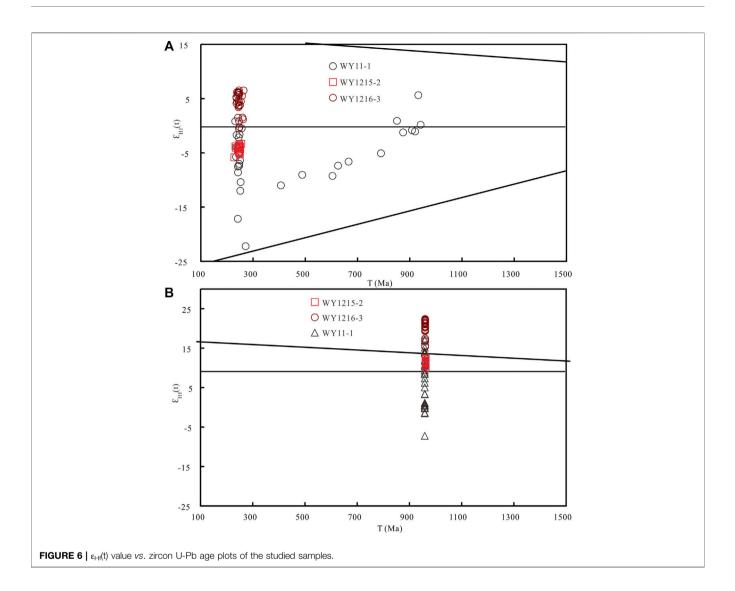
lower intercept age of 246 ± 6 Ma. The zircon grains with ages of ~246 Ma show uniformly low Th/U ratios while those with older ages have high Th/U ratios (**Figure 5** and **Supplementary Table S3**), which imply their metamorphic and magmatic origins. These results are consistent with previous studies that the high-grade metamorphism occurred during the Early Triassic (Zhao L. et al., 2017; Xia et al., 2021).

Zircon O-Hf Isotopic Compositions

The zircon grains of the two retrograded eclogite samples show significant differences in O isotopic compositions (**Supplementary Table S4** and **Figure 5**). The $\delta^{18}O$ (V-SMOW) values are 3.85–6.08 for zircons from the sample WY1215-2, and 8.46–11.34 for those of

the sample WY1216-3. The distinct O isotopic compositions of these metamorphic zircons suggest zircon precipitation from different metamorphic fluids. The $\delta^{18}O$ (V-SMOW) values of zircon cores and rims from the mafic granulite sample show large variations, with cores having low $\delta^{18}O$ values of ~5.5 while rims having high $\delta^{18}O$ values around ~8 (**Supplementary Table S4** and **Figure 5**).

The zircon Hf isotopic compositions of the two retrograded eclogite samples are relatively homogenous, with $^{176}Hf/^{177}Hf$ ratios of 0.282646–0.282521 for WY1215-1 and of 0.281223–0.282806 for WY1216-2 (mostly within the range of 0.282605–0.282798, **Supplementary Table S5**). $\varepsilon_{Hf}(t)$ values are all negative for zircons from the sample WY1215-1 (ranging from −5.9 to −3.4) and mostly positive for zircons from the sample WY1216-2 (ranging

FIGURE 6 | $\varepsilon_{Hf}(t)$ value *vs.* zircon U-Pb age plots of the studied samples.

from −16.1 to +6.6, mostly ranging from 0.9 to 6.6). The single-stage depleted mantle model ages of the sample WY1215-1 are 1011–1088 Ma and 619–2787 Ma (mostly within the range of 619–892 Ma). For the reason that the zircons from the granulite sample exhibit complex internal structures, their Hf isotopic compositions also show large variations, with $^{176}Hf/^{177}Hf$ ratios ranging from 0.281980 to 0.282654 and related $\varepsilon_{Hf}(t)$ values ranging from −22 to +5.6 (**Supplementary Table S5**). The single-stage depleted mantle model ages are 829–1772 Ma. In the zircon U-Pb age *vs.* $\varepsilon_{Hf}(t)$ value diagram, the analyzed results plot above and below the CHUR evolutionary line, based on calculations using apparent zircon U-Pb ages (**Figure 6**). However, if using the protolith age of the mafic granulite (~960 Ma) as the starting age, $\varepsilon_{Hf}(t)$ values of most analyses plot above the CHUR evolutionary line (**Figure 6**).

Whole-Rock Sm-Nd Isotopic Compositions

The six analyzed samples show quite different whole-rock Sm-Nd isotopic compositions (**Supplementary Table S6**). The retrograded eclogite have higher $^{143}Nd/^{144}Nd$ ratios

(0.512487–0.512694) than the granulite samples (0.511343–0.512144). The single-stage depleted mantle model ages are mostly Mesoproterozoic for the retrograded eclogite samples (1360–1790 Ma), except one sample with an Archean model age of ~2620 Ma, while those of the mafic granulite samples are older, at 1860–3020 Ma. The $\varepsilon_{Nd}(t)$ values (assuming that the protolith ages are Neoproterozoic based on the protolith age of the mafic granulite, Zhao L. et al., 2017) of the retrograded eclogite samples are positive, ranging from 1.94 to 5.46 while those of the two mafic granulite samples are negative, one at −1.35 and the other at −7.74.

DISCUSSIONS

Indosinian Metamorphism in and Around the SCB

As mentioned earlier, the Indosinian orogeny affected large areas of the SCB. Although previous studies claimed that many of the Neoproterozoic sequences belonging to the Banxi Group
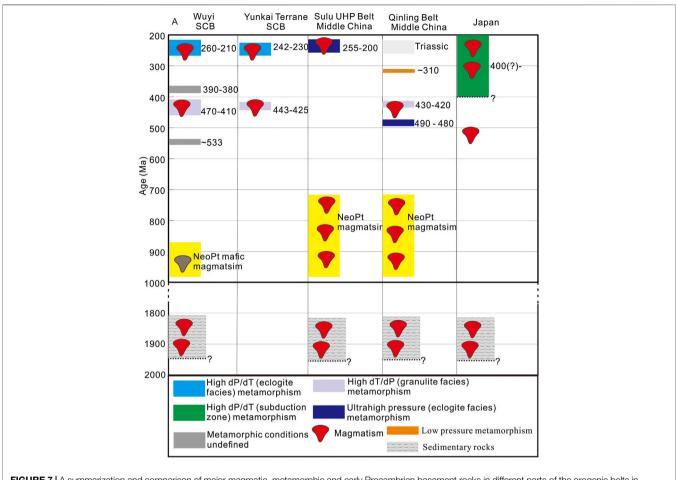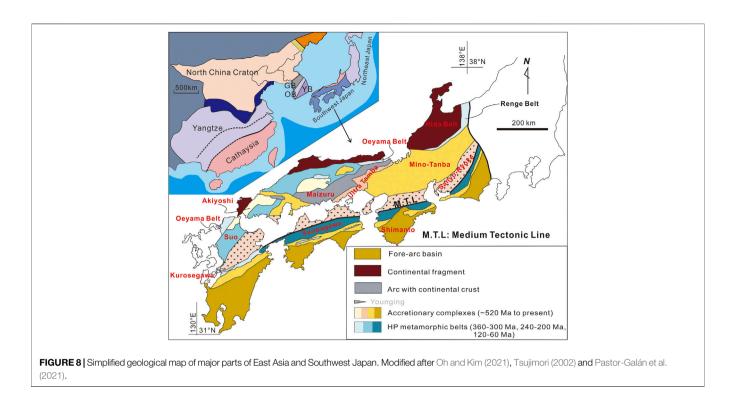
FIGURE 7 | A summarization and comparison of major magmatic, metamorphic and early Precambrian basement rocks in different parts of the orogenic belts in and around the SCB. Related references can be found in the main text.

represent the Precambrian basement of the SCB, Indosinian reworking of these sequences are significant, represented by folding, shearing and long-distance thrusting within the Jiangnan belt (Chu et al., 2012a; Chu et al., 2012b; Chu et al., 2012c; Liu L. et al., 2012; Wang Y. et al., 2005). These deformation features are typical of thin-skinned tectonics, involving only upper crustal components. The occurrences of the high-grade rocks in the northern Wuyi terrane suggest that the orogeny of this region affected deep lower crustal components. The peak pressure conditions of the retrograded eclogite samples indicate the crustal thickness of the northern Wuyi terrane was almost doubled during the orogeny. The decompressional reaction textures and the isothermal (or slow heating) decompressional P-T stage in the P-T trajectories imply that the orogenic belt experienced quick collapse and the high-grade rocks experienced fast uplifting during the late thermal relaxation stage (**Figure 3**, Zhao L. et al., 2017). The metamorphic features of these high-grade rocks are strongly reminiscent of those found in plate margin contractional settings (Brown, 2009; O'Brien, 1993). New SIMS zircon U-Pb dating results confirm the time of metamorphism at 246–249 Ma (**Figure 5**). Indosinian metamorphism has also been reported from the Yunkai

terrane in the southwestern Cathaysia Block (**Figures 1**, **7**, Chen C.-H. et al., 2012; Lin et al., 2008; Wan et al., 2010). However, the occurrences of Indosinian metamorphism are not continuous from the Wuyi terrane to the Yunkai terrane, implying that they might not belong to the same Indosinian orogenic belt. Tectonic geometry as well as metamorphic features of the Yunkai terrane exhibit close affinities to the Indosinian tectonothermal events in southwestern SCB and Indochina, which are inconsistent with those of the Wuyi terrane (Lin et al., 2008; Faure et al., 2014; Faure et al., 2016a; Faure et al., 2016b).

The Indosinian high-grade metamorphism in east Eurasia that attracted the most international interests occurs along the Central China Orogenic belt, which is further divided into small segments of the Qinling, Tongbai, Hong'an, Dabie and Sulu (**Figure 1**). This composite orogenic belt records the complete amalgamation history of the two major continental parts of east Eurasia, namely the SCB and the North China Craton, and besides, the identification of ultrahigh-pressure metamorphic minerals like coesite and diamond from eclogites with continental crustal chemical compositions imply deep subduction of the SCB continental crust (Dong et al., 2016; Okay and Celal Şengör,

FIGURE 8 | Simplified geological map of major parts of East Asia and Southwest Japan. Modified after Oh and Kim (2021), Tsujimori (2002) and Pastor-Galán et al. (2021).

1992; Wang et al., 1989; Wu and Zheng, 2013; Xu et al., 1992; Zhai et al., 1995; Zhao Z.-F. et al., 2017). Multiple geochronological studies constrain the time of eclogite facies metamorphism of the Sulu and Dabie segments to be at 255–200 Ma, mostly Triassic (**Figure 7**, An et al., 2018; Cheng et al., 2011; Li S. et al., 2017; Liu et al., 2004, Liu et al., 2006; Wu and Zheng, 2013), synchronous with these of the Wuyi terrane. As to the Qinling segment of the Central China Orogenic belt, its high-grade metamorphism occurred mainly during Paleozoic and Triassic overprintings are not very strong (**Figure 7**, Dong et al., 2011). The influence of such an extreme contractional orogen is significant and many of the Indosinian metamorphic events in East Asia have been correlated with this orogenic belt, like those in the Korean Peninsula and Japan (Kwon et al., 2009; Liu, 1993; Oh and Kim, 2021; Ree et al., 1996; Tsujimori, 2002; Ernst et al., 2007). As shown in **Figure 1**, the striking direction of the Sulu segment of the Central China Orogenic belt is parallel with the Indosinian orogenic belt in the Wuyi terrane of the Cathaysia Block, both following northeast-southwest direction. Almost synchronously, the collision between the SCB and the Indochina Peninsula resulted in high-grade metamorphism in southwest SCB and also Indochina (Faure et al., 2014, 2016a, b), whose major tectonic geometry is, however, mainly northwest-southeast (Faure et al., 2016b).

Another important plate that greatly affected the Phanerozoic SCB and which has been overlooked in many previous studies is the one facing its southeastern continental margin, the Paleo-Pacific plate (**Figure 1**). Although still controversial, many geologists suggested the onset of the SCB active continental margin facing the Pacific plate during Mesozoic (Zhou and Li, 2000; Zhou et al., 2006), or during Paleozoic (Li et al., 2006; Li and

Li, 2007; Sun et al., 2011). However, pre-Triassic geological records of interactions with the Pacific oceanic plate are now absent in the southeastern SCB continental margin, which is mainly composed of late Mesozoic magmatic rocks (volcanics and intrusive rocks, Shu, 2012; Xu et al., 2007). The Japanese islands, which preserve various geological records of oceanic subduction, accretion, subduction erosion and the formation of the continental crust due to interactions with the Pacific plate, ranging from Paleozoic to Cenozoic, have been suggested to show consanguineous with the SCB (**Figure 8**, Taira, 2001; Wakita, 2013; Pastor-Galán et al., 2021; Isozaki et al., 2010; Wallis et al., 2020). Indeed some of the early Precambrian lithologies in the Hida belt of Southwest Japan show consanguineous with those of the North China Craton as previously suggested (**Figure 8**, Horie et al., 2010; Kawabata et al., 2021; Harada et al., 2021a, 2021b; Kimura et al., 2019), but these sporadically occurred Paleoproterozoic intrusive rocks (~1.85 Ga) as well as the Archean-Paleoproterozoic detrital and/or inherited zircon grains are also comparable to those of the Badu Complex in the Wuyi terrane of the Cathaysia Block (Li et al., 2014; Yu et al., 2009, 2012; Zhao et al., 2015; Isozaki, 2019). Besides, the Paleozoic (~450–410 Ma) and/or Indosinian metamorphic overprintings, as well as the Neoproterozoic lithologies of the Wuyi terrane in northeast Cathaysia Block also provide arguments for a close consanguinity of Japan with the SCB (Zhao et al., 2016, Zhao et al., 2020; Xu et al., 2007; Shu et al., 2008a, Shu et al., 2008b; Horie et al., 2010; Kimura et al., 2019; Harada et al., 2021b). These correlations support the inference that the ancient continental fragments preserved in Japan probably originated from the SCB (Aoki et al., 2015; Isozaki et al., 2010, Isozaki et al., 2014; Tsutsumi

et al., 2017; Isozaki, 2019; Pastor-Galán et al., 2021). Besides, the Paleozoic and Mesozoic geological components, like the Paleozoic accretionary complexes, the Mesozoic accretionary complexes, as well as the arc batholiths and ophiolitic mélange in Japan, are quite likely to be the missing continental marginal components of the SCB during the Indosinian orogeny(Isozaki et al., 2010, Isozaki et al., 2014; Isozaki, 2019; Pastor-Galán et al., 2021). Metamorphism of the Japanese islands are mainly low-temperature, high-pressure subduction type and continuous from Paleozoic onwards (**Figure 7**, Ishiwatari and Tsujimori, 2003; Erst et al., 2007; Matsunaga et al., 2021; Takahashi et al., 2018; Tsujimori, 2002; Tsujimori et al., 2006; Tsujimori and Liou, 2004). Alongside with these subduction zone metamorphism, the low (and medium) dP/dT metamorphism can also often be seen (Takahashi et al., 2018), which collectively termed as the 'paired metamorphic belts' (Miyashiro, 1961, 1973). One thing worthy of noticing is the preservation of geological records for an accreted oceanic plateau in Southwest Japan (Tatsumi et al., 2000). These geological records are critical for a better understanding the geological history of the Phanerozoic SCB.

Characteristics of the Protoliths of the High-Grade Rocks

The eclogite and granulite facies mineral assemblages indicate that the studied mafic rocks experienced high-grade metamorphism which might render their whole-rock chemical compositions unreliable, especially the major elements and the fluid-mobile elements like Th, K, etc. The large spread of these samples in **Figure 4A** partly attests to this inference. However, some overall variation trends can still be extracted from the relatively immobile element plots (**Figure 4**), like their sub-alkaline basaltic and tholeiitic compositions. They show close affinities to oceanic crust, with the retrograded eclogite samples resembling E-MORB while the mafic granulite samples resembling OIB. The protoliths of these rocks, therefore, are interpreted to represent the remnants of a disappeared ocean.

Zircon O-Hf isotopic compositions of these metamorphosed mafic rocks exhibit large variations as well, but the magmatic zircon cores preserved in the mafic granulite sample have mantle-like O isotopic signatures (**Figure 5**, Valley et al., 1994). The Neoproterozoic age of 946 Ma constrained by these magmatic zircon cores is interpreted to represent the protolith age of the mafic granulite. Both the zircon Lu-Hf and whole-rock Sm-Nd isotopic compositions of these mafic rocks show large variations. Considering that the hosting rocks of these mafic rocks are the Paleoproterozoic sedimentary rocks of the Badu Complex, any influence from which during high-grade metamorphism will elevate model ages while lowering ε(t) values for both Lu-Hf and Sm-Nd isotopic systems, the high-grade samples of this study with the youngest single-stage model ages and the highest ε (t) values should be regarded to give the best constraints on the features of these meta-mafic rocks. As described above, the youngest single-stage Hf model ages for both the retrograded eclogite and mafic granulite samples are Neoproterozoic, 619–892 Ma for the retrograded eclogite, and 829—~1000 Ma for the mafic granulite. Whole-rock Sm-Nd isotopic
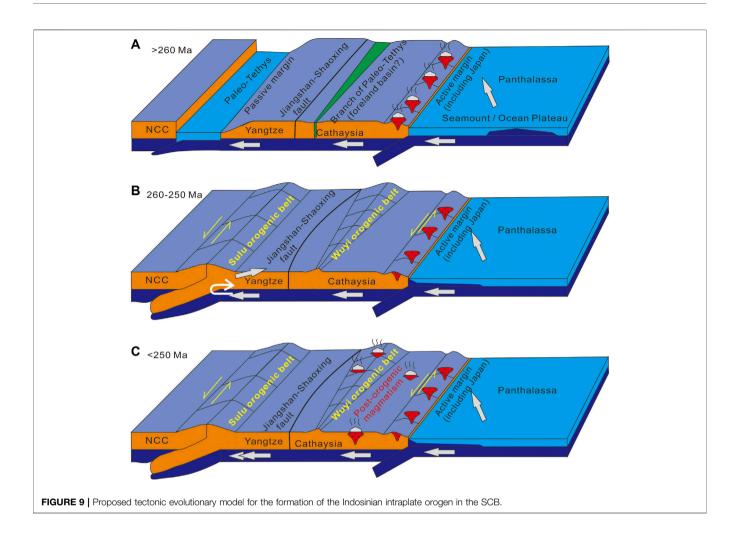
compositions for these high-grade rocks seem to have been disturbed during metamorphism because they exhibit large variations on one hand and on the other hand, the single-stage model ages are Mesoproterozoic to Archean, significantly older than the Hf model ages. The Neoproterozoic protolith ages (990–950 Ma) for these metamorphosed mafic blocks are, therefore, supported by both the magmatic zircon core U-Pb age of the mafic granulite, and the Hf - Nd isotopic compositions.

Previous studies have revealed the occurrences of two episodes of Neoproterozoic magmatism in the Cathaysia Block, one at ~970 Ma and the other at 860–800 Ma (Shu et al., 2008a; Shu et al., 2011; Wang Y. et al., 2014). They have been interpreted to occur in the active continental margin and within plate rifting environments, respectively (Shu et al., 2008a; Shu et al., 2011). If taking the zircon core age of ~950 Ma as the protolith age, the metamorphosed blocks of this study can correlate well with the ~970 Ma magmatism in the Cathaysia Block, representing continental margin components. The protoliths of these metamorphosed mafic blocks, generated during Neoproterozoic, can also be compared with the widespread Neoproterozoic lithologies in the Jiangnan belt (Wang et al., 2013b; Wang Y. et al., 2014; Yao et al., 2014). All these Neoproterozoic magmatic rocks are related to the tectonothermal events that amalgamated the Yangtze and Cathaysia Blocks, and the subsequent rifting (Nanhua Rift) (Li et al., 2009a; Li W. X. et al., 2010; Wang X.-L. et al., 2012). Anyway, the Neoproterozoic magmatic rocks are important components of the continental crust of the SCB during the Indosinian orogeny, rather than newly generated oceanic crustal component (Yu et al., 2008; Shu, 2006, 2012).

Formation of the Indosinian SCB Intraplate Orogenic Belt and Broad International Implications

If based solely on the Indosinian high-grade metamorphism of the Wuyi terrane in northeastern Cathaysia Block, the conclusion of a continental margin orogenic belt can be assigned to the SCB Indosinian orogen, because these metamorphic rocks show identical features with those developed in continental margin orogenic belts (Brown, 2009; O'Brien, 1993). But the geological implications of high-grade metamorphism are not always exclusive and as pointed out by Raimondo et al. (2014), the crustal shortening and thickening, and exhumation high-grade metamorphic rocks from deep crustal levels of intraplate orogens are comparable with their plate-margin counterparts. Therefore, the eclogite and the granulite facies metamorphism such as these of the Wuyi terrane could suggest both intraplate and plate marginal settings.

The spatial occurrence of orogenic metamorphism has been suggested to be a powerful tool in discriminating styles of orogens (Raimondo et al., 2014; Zhai, 2009; Li et al., 2016c, Li et al., 2016d). As summarized by Zhao et al. (2015) and shown in **Figure 1**, the occurrences of the Indosinian high-grade metamorphism are found to occur only in the northeastern Cathaysia Block (Wuyi terrane) and are absent in the Nanling area. In other words, their distribution is not continuous and does

FIGURE 9 | Proposed tectonic evolutionary model for the formation of the Indosinian intraplate orogen in the SCB.

not form a complete belt that can demarcate the continental boundaries. Such a distribution pattern of high-grade metamorphism is inconsistent with those developed in continental marginal settings, but rather indicates an intracontinental setting. Besides the mafic blocks studied in this paper which show continental crust characteristics, other lithologies in the Cathaysia Block exhibiting Indosinian high-grade metamorphic alterations mainly belong to the Paleoproterozoic Badu and Mayuan Complexes of the Wuyi terrane (Yu et al., 2012; Zhao et al., 2015; Zhao L. et al., 2018). The occurrences of all these rocks indicate that the Indosinian orogeny affected only the ancient continental crust components, without the addition of any juvenile components newly generated from mantle which is, however, usually normal for continental marginal orogenic belts due to the consumption of oceanic crust before the final collision (e.g. Jamieson and Beaumont, 2013; Li et al., 2016e; Hou et al., 2021). In summary, although the high-grade rocks in the Wuyi terrane record metamorphism similar to those seen in continental margin settings, they are more likely to have occurred in the intracontinental environment.

The development of intracontinental orogens normally requires the existence of weak lithospheric zones within the continental block (Collins et al., 2011; Raimondo et al., 2014; Sokoutis and Willingshofer, 2011). As mentioned earlier, a Neoproterozoic rifted system termed the Nanhua rift developed in the SCB, as indicated by the wide occurrences of Neoproterozoic magmatism (860–800 Ma) (Shu et al., 2008a, Shu et al., 2011; Li et al., 2005; Wang and Li, 2003; Wang et al., 2007). This rift system is also known to be a failed rift because it aborted soon afterwards and no new ocean was developed. The South China Caledonian orogeny should have solidified most of the failed rift and formed another basin (foreland?) in the Wuyi terrane which behaved as a branch of the Paleo-Tethys Ocean and provided the weak lithospheric zone in the Cathaysia Block (**Figure 9A**). Another critical cause of the intraplate orogen is the driving force. Stress source of orogenic belts, either occurring in the intraplate or plate margin settings, are originally derived from the viscous mantle convections, which operate as conveyors and transport the lithosphere to different places of the Earth, resulting in the formation of convergent and divergent plate margins (Collins, 2003; Collins et al., 2011). The driving forces of intraplate orogens have been more specifically suggested to include far-field stress from plate margins, and intraplate stress largely related to vertical tectonic processes (Raimondo et al., 2014). The geometry of the Indosinian orogen is

inconsistent with intraplate stress and implies stress sources from continental margins. The mantle convection cell in the Paleo-Tethys tectonic realm transported the SCB northward (today's orientation), closing the Paleo-Tethys Ocean and forming the Central China Orogenic belt during Permo-Triassic (Collins et al., 2011; Ratschbacher et al., 2003; Wu and Zheng, 2013). The subduction of the paleo-Pacific plate underneath the SCB (including Japan) during the Paleozoic represents another mantle convection cell with a northwestward (today's orientation) conveying direction (**Figure 9A**, Li et al., 2006; Li and Li, 2007). Previous studies on the Indosinian deformation and magmatic activities of the SCB revealed that during ~260–250 Ma, an oceanic plateau arrived at the subduction zone which choked the magmatic arc and besides, the stress, that used to localize on the southeastern continental margin of the SCB, propagated from the continental margin northwestward to inland regions (**Figure 9B**, Li and Li, 2007; Tatsumi et al., 2000). Based on these discussions, we suggest that the far-field stress from the southeast margin of the SCB due to interactions with the paleo-Pacific plate must have facilitated the formation of the SCB Indosinian intraplate orogen. The spatial distribution of the Indosinian high-grade metamorphism in the Cathaysia Block is parallel with the Sulu orogenic belt (**Figure 1**) and the metamorphic ages of the high-grade rocks within these two orogenic belts greatly overlap (**Figure 7**), implying that this segment of the Central China Orogenic belt along the northern margin of the SCB is another stress source for the Indosinian intraplate orogeny of the SCB (**Figure 9B**). This inference is consistent with previous studies which have already proposed that the Indosinian orogeny of the SCB is closely related to the far-field stress from the Central China Orogenic belt (Zhang et al., 2013; Li J. et al., 2017; Wang et al., 2021).

A complete model for the formation of the Indosinian intraplate orogen in the SCB is, therefore, proposed based on the above discussions (**Figure 9**). After the amalgamation of the Yangtze and Cathaysia Blocks during Neoproterozoic, the SCB soon witnessed rifting and formed the Nanhua Rift (Li W. X. et al., 2010; Li et al., 2005; Wang X.-C. et al., 2012, Wang X.-L. et al., 2012). This rift system aborted soon afterwards without the formation of open oceans. During Paleozoic, the South China Caledonian orogeny closed solidified this rift system and likely formed a foreland basin in the Cathaysia Block which remained there until Permo-Triassic (**Figure 9A**, Shu et al., 2008a; Shu et al., 2011), providing the lithospheric weak zone for the intraplate orogenic events. The onset of the active continental margin of the SCB facing the paleo-Pacific (Panthalassa) plate dates back to the Paleozoic and during Permo-Triassic, the arrival of an oceanic plateau at the subduction zone choked the magmatic arc and the stress propagated to the inland regions of the SCB. Almost simultaneously, the collisional events between the SCB and the North China Craton slowed the northward moving of the SCB, providing another retroactive stress source to the SCB (**Figure 9B**). Therefore, stress from both the northwest (Sulu orogenic belt) and southwest (paleo-Pacific) margins during Permo-Triassic acted within the SCB, forming a super-contraction zone in the Wuyi terrane of the northeast Cathaysia Block. The weak lithospheric zone of the Cathaysia Block accommodated the strain and witnessed strong deformation and significant crustal thickening, termed as the Indosinian Wuyi orogenic belt (**Figure 9B**). After the collision of the SCB with the North China Craton, the major driving force for the convergence of these two continental blocks is believed to be the dragging of the eclogitized mafic crust of northern South China (Dong et al., 2013), providing an extensional environment in the Cathaysia Block which resulted in orogenic collapse and the formation of post-orogenic magmatism (**Figure 9C**, Li W. et al., 2012; Sun et al., 2011, Sun et al., 2017). This new model is not only consistent with the geological records in and around the SCB but also has geological implications for interpreting intraplate orogens worldwide.

CONCLUSION

Based on the above descriptions and discussions, the following conclusions can be reached.

1) The occurrences of the Indosinian high-grade metamorphism define the northeast-southwest trending orogenic belt in the Cathaysia Block, southeast SCB, representing the uplifted Indosinian orogenic core components.

2) Whole-rock major and trace element compositions of the high-grade rocks vary significantly, due to metamorphic alterations. The overall trend of their variations constrains the protoliths to be emplaced in plate margin settings, showing E-MORB and OIB compositions by relatively immobile elements.

3) SIMS zircon U-Pb age dating confirm the metamorphic age of 246–249 Ma and an early Neoproterozoic protolith age of 946 Ma. The magmatic zircon cores still preserve mantle-like O isotopic compositions of ~5.5 (δ^{18}O (V-SMOW)). Metamorphic zircons exhibit large variations in O isotopic compositions. Compared with whole-rock Sm-Nd isotopic compositions, zircon Lu-Hf isotopic compositions can better trace the features of the protoliths, confirming their generation during the early Neoproterozoic.

4) The protoliths of these metamorphic rocks were generated during the early Neoproterozoic and were continental crustal components during the Indosinian orogeny. Combined with the spatial distributions of the Indosinian metamorphism in the Cathaysia Block, we suggest that this orogen formed in the intraplate environment.

5) A summarization of Indosinian plate margin activities of the SCB led us to conclude that the driving stress for the formation of the SCB Indosinian orogen in the Wuyi terrane is from both the interactions with the paleo-Pacific plate in the southeast and the North China Craton in the north. In other words, the mantle convection cell that closed the Paleo-Tethys, and the one conveying the paleo-Pacific plate to the SCB continental margin both facilitated the formation of the Indosinian orogen in the Wuyi terrane of the Cathaysia Block. This Indosinian intraplate orogenic belt was primarily a lithospheric weak zone formed during the South China Caledonian orogeny.

DATA AVAILABILITY STATEMENT

The original contributions presented in the study are included in the **Supplementary Material**, further inquiries can be directed to the corresponding author.

AUTHOR CONTRIBUTIONS

LZ carried out all the analyses, processed the data and wrote the manuscript. MZ the leader of the research project, planned the blueprint of the research and provided corrections on the different versions of the manuscript. XZ Initiated the research, funded the field trip and the lab work, and helped preparing the manuscript.

FUNDING

ACKNOWLEDGMENTS

SUPPLEMENTARY MATERIAL

The Supplementary Material for this article can be found online at: https://www.frontiersin.org/articles/10.3389/feart.2022.892787/full#supplementary-material

Supplementary Table S1 | Information of the studied samples of this study.

Supplementary Table S2 | Whole-rock geochemical compositions of the studied samples.

Supplementary Table S3 | SIMS zircon U-Pb age dating results of the studied samples.

Supplementary Table S4 | SIMS zircon O isotope results of the studied samples.

Supplementary Table S5 | Zircon Lu-Hf isotopic compositions of the studied samples.

Supplementary Table S6 | Whole-rock Sm-Nd isotopic compositions of the studied samples.

REFERENCES

An, S.-C., Li, S.-G., and Liu, Z. (2018). Modification of the Sm-Nd Isotopic System in Garnet Induced by Retrogressive Fluids. *J. Metamorph Geol.* 36, 1039–1048. doi:10.1111/jmg.12426

Aoki, K., Isozaki, Y., Yamamoto, A., Sakata, S., and Hirata, T. (2015). Mid-Paleozoic Arc Granitoids in SW Japan with Neoproterozoic Xenocrysts from South China: New Zircon U-Pb Ages by LA-ICP-MS. *J. Asian Earth Sci.* 97, 125–135. doi:10.1016/j.jseaes.2014.10.018

Blichert-Toft, J., and Albarède, F. (1997). The Lu-Hf Isotope Geochemistry of Chondrites and the Evolution of the Mantle-Crust System. *Earth Planet. Sci. Lett.* 148, 243–258. doi:10.1016/s0012-821x(97)00040-x

Brown, M. (2009). Metamorphic Patterns in Orogenic Systems and the Geological Record. *Geol. Soc.* 318, 37–74. doi:10.1144/sp318.2

Chen, C.-H., Liu, Y.-H., Lee, C.-Y., Xiang, H., and Zhou, H.-W. (2012a). Geochronology of Granulite, Charnockite and Gneiss in the Poly-Metamorphosed Gaozhou Complex (Yunkai Massif), South China: Emphasis on the *In-Situ* EMP Monazite Dating. *Lithos* 144-145, 109–129. doi:10.1016/j.lithos.2012.04.009

Chen, D. F., Li, X. H., Pan, J. M., Dong, W. Q., Chen, G. Q., and Chen, X. P. (1998). Metamorphic Newly Produced Zircons, SHRIMP Ion Microprobe U-Pb Age of Amphibolite of Hexi Group, Zhejiang and its Implications. *Acta Mineral. Sin.* 18, 396–400.

Chen, J., Foland, K. A., Xing, F., Xu, X., and Zhou, T. (1991). Magmatism along the Southeast Margin of the Yangtze Block: Precambrian Collision of the Yangtze and Cathysia Blocks of China. *Geology* 19, 815–818.

Chen, X., Fan, J., Chen, Q., Tang, L., and Hou, X. (2014). Toward a Stepwise Kwangsian Orogeny. *Sci. China Earth Sci.* 57, 379–387. doi:10.1007/s11430-013-4815-y

Chen, X., Tong, L., Zhang, C., Zhu, Q., and Li, Y. (2015). Retrograde Garnet Amphibolite from Eclogite of the Zhejiang Longyou Area: New Evidence of the Caledonian Orogenic Event in the Cathaysia Block. *Chin. Sci. Bull.* 60, 1207–1217. doi:10.1007/s11434-015-0890-0

Chen, X., Zhang, Y., Fan, J., Tang, L., and Sun, H. (2012b). Onset of the Kwangsian Orogeny as Evidenced by Biofacies and Lithofacies. *Sci. China Earth Sci.* 55, 1592–1600. doi:10.1007/s11430-012-4490-4

Cheng, H., Zhang, C., Vervoort, J. D., Wu, Y., Zheng, Y., Zheng, S., et al. (2011). New Lu-Hf Geochronology Constrains the Onset of Continental Subduction in the Dabie Orogen. *Lithos* 121, 41–54. doi:10.1016/j.lithos.2010.10.004

Chu, Y., Faure, M., Lin, W., and Wang, Q. (2012a). Early Mesozoic Tectonics of the South China Block: Insights from the Xuefengshan Intracontinental Orogen. *J. Asian Earth Sci.* 61, 199–220. doi:10.1016/j.jseaes.2012.09.029

Chu, Y., Faure, M., Lin, W., Wang, Q., and Ji, W. (2012b). Tectonics of the Middle Triassic Intracontinental Xuefengshan Belt, South China: New Insights from Structural and Chronological Constraints on the Basal Décollement Zone. *Int. J. Earth Sci. Geol. Rundsch)* 101, 2125–2150. doi:10.1007/s00531-012-0780-5

Chu, Y., Lin, W., Faure, M., Wang, Q., and Ji, W. (2012c). Phanerozoic Tectonothermal Events of the Xuefengshan Belt, Central South China: Implications from UPb Age and LuHf Determinations of Granites. *Lithos* 150, 243–255. doi:10.1016/j.lithos.2012.04.005

Collins, W. J., Belousova, E. A., Kemp, A. I. S., and Murphy, J. B. (2011). Two Contrasting Phanerozoic Orogenic Systems Revealed by Hafnium Isotope Data. *Nat. Geosci.* 4, 333–337. doi:10.1038/ngeo1127

Collins, W. J. (2003). Slab Pull, Mantle Convection, and Pangaean Assembly and Dispersal. *Earth Planet. Sci. Lett.* 205, 225–237. doi:10.1016/s0012-821x(02)01043-9

Cui, S., and Li, J. (1983). On the Indosinian Movement of China's Peri-Pacific Tectonic Belt. *Acta Geol. Sin.* 1, 51–62.

Dong, S., Gao, R., Yin, A., Guo, T., Zhang, Y., Hu, J., et al. (2013). What Drove Continued Continent-Continent Convergence after Ocean Closure? Insights from High-Resolution Seismic-Reflection Profiling across the Daba Shan in Central China. *Geology* 41, 671–674. doi:10.1130/g34161.1

Dong, Y., Safonova, I., and Wang, T. (2016). Tectonic Evolution of the Qinling Orogen and Adjacent Orogenic Belts. *Gondwana Res.* 30, 1–5. doi:10.1016/j.gr.2015.12.001

Dong, Y., Zhang, G., Neubauer, F., Liu, X., Genser, J., and Hauzenberger, C. (2011). Tectonic Evolution of the Qinling Orogen, China: Review and Synthesis. *J. Asian Earth Sci.* 41, 213–237. doi:10.1016/j.jseaes.2011.03.002

Ernst, W. G., Tsujimori, T., Zhang, R., and Liou, J. G. (2007). Permo-Triassic Collision, Subduction-Zone Metamorphism, and Tectonic Exhumation along the East Asian Continental Margin. *Annu. Rev. Earth Planet. Sci.* 35, 73–110. doi:10.1146/annurev.earth.35.031306.140146

Faure, M., Charvet, J., and Chen, Y. (2018). Appalachian-style Multi-Terrane Wilson Cycle Model for the Assembly of South China: COMMENT. *Geology* 46, e446. doi:10.1130/g40222c.1

Faure, M., Lepvrier, C., Nguyen, V. V., Vu, T. V., Lin, W., and Chen, Z. (2014). The South China Block-Indochina Collision: where, when, and How? *J. Asian Earth Sci.* 79, 260–274. doi:10.1016/j.jseaes.2013.09.022

Faure, M., Lin, W., Chu, Y., and Lepvrier, C. (2016a). Triassic Tectonics of the Ailaoshan Belt (SW China): Early Triassic Collision between the South China and Indochina Blocks, and Middle Triassic Intracontinental Shearing. *Tectonophysics* 683, 27–42. doi:10.1016/j.tecto.2016.06.015

Faure, M., Lin, W., Chu, Y., and Lepvrier, C. (2016b). Triassic Tectonics of the Southern Margin of the South China Block. *Comptes Rendus Geosci.* 348, 5–14. doi:10.1016/j.crte.2015.06.012

Grabau, A. (1924). *Stratigraphy of China, Part I, Paleozoic and Older. 1-528.* Peking: Geological Survey and Ministry of Agriculture and Commerce of China.

Griffin, W. L., Wang, X., Jackson, S. E., Pearson, N. J., O'Reilly, S. Y., Xu, X., et al. (2002). Zircon Chemistry and Magma Mixing, SE China: *In-Situ* Analysis of Hf Isotopes, Tonglu and Pingtan Igneous Complexes. *Lithos* 61, 237–269. doi:10.1016/s0024-4937(02)00082-8

Guo, L. Z., Shi, Y. S., Ma, R. S. Y., Shang, F., and Lu, H. F. (1984). Tectonostratigraphic Terranes of Southeast China. *J. Nanjing Univ. Nat. Sci. Ed.* 20, 732–739.

Gupta, S., Rodgers, J., Hsü, K. J., Shu, S., Jiliang, L., Haihong, C., et al. (1989). Comments and Reply on "Mesozoic Overthrust Tectonics in South China". *Geol* 17, 669–673. doi:10.1130/0091-7613(1989)017<0669:caromo>2.3.co;2

Hand, M., and Sandiford, M. (1999). Intraplate Deformation in Central Australia, the Link between Subsidence and Fault Reactivation. *Tectonophysics* 305, 121–140. doi:10.1016/s0040-1951(99)00009-8

Harada, H., Tsujimori, T., Kon, Y., Aoki, S., and Aoki, K. (2021a). Nature and Timing of Anatectic Event of the Hida Belt (Japan): Constraints from Titanite Geochemistry and U-Pb Age of Clinopyroxene-Bearing Leucogranite. *Lithos*, 398–399. doi:10.1016/j.lithos.2021.106256

Harada, H., Tsujimori, T., Kunugiza, K., Yamashita, K., Aoki, S., Aoki, K., et al. (2021b). The δ^{13}C – δ^{18}O Variations in Marble in the Hida Belt, Japan. *Isl. Arc* 30. doi:10.1111/iar.12389

Horie, K., Yamashita, M., Hayasaka, Y., Katoh, Y., Tsutsumi, Y., Katsube, A., et al. (2010). Eoarchean-Paleoproterozoic Zircon Inheritance in Japanese Permo-Triassic Granites (Unazuki Area, Hida Metamorphic Complex): Unearthing More Old Crust and Identifying Source Terrranes. *Precambrian Res.* 183, 145–157. doi:10.1016/j.precamres.2010.06.014

Hou, Q.-L., Guo, Q.-Q., Chen, Y.-C., Cheng, N.-N., Shi, M.-Y., and Li, J.-L. (2021). Discussions on the Mountains and Orogenic Belts and Related Issues. *Acta Petrol. Sin.* 37, 2287–2302. doi:10.18654/1000-0569/2021.08.02

Hsü, K. J. (1989). Geotectonic Structure of South China and its Relations with Japan. *Prog. Earth Sci.* 01, 22–27.

Hsü, K. J., Li, J., Chen, H., Wang, Q., Sun, S., and Sengör, A. (1990). Tectonics of South China: Key to Understanding West Pacific Geology. *Tectonophysics* 183, 9–39.

Hsü, K. J., Sun, S., Li, J., Chen, H., Pen, H., and Sengor, A. (1988). Mesozoic Overthrust Tectonics in South China. *Geology* 16, 418–421.

Hu, S. X., and Ye, Y. (2006). Questions to 'Cathaysia Oldland', 'Cathaysia Block' and 'United Yangtze-Cathaysia Oldland' of South China. *Geol. J. China Univ.* 12, 432–439.

Huang, J. Q. (1984). New Researches on the Tectonic Characteristics of China. *Bull. Chin. Acad. Geol. Sci.* 9, 5.

Irvine, T. N., and Baragar, W. R. A. (1971). A Guide to the Chemical Classification of the Common Volcanic Rocks. *Can. J. Earth Sci.* 8, 523–548. doi:10.1139/e71-055

Ishiwatari, A., and Tsujimori, T. (2003). Paleozoic Ophiolites and Blueschists in Japan and Russian Primorye in the Tectonic Framework of East Asia: A Synthesis. *Isl. Arc* 12, 79–206. doi:10.1046/j.1440-1738.2003.00390.x

Isozaki, Y. (2019). A Visage of Early Paleozoic Japan: Geotectonic and Paleobiogeographical Significance of Greater South China. *Isl. Arc* 28. doi:10.1111/iar.12296

Isozaki, Y., Aoki, K., Nakama, T., and Yanai, S. (2010). New Insight into a Subduction-Related Orogen: A Reappraisal of the Geotectonic Framework and Evolution of the Japanese Islands. *Gondwana Res.* 18, 82–105. doi:10.1016/j.gr.2010.02.015

Isozaki, Y., Aoki, K., Sakata, S., and Hirata, T. (2014). The Eastern Extension of Paleozoic South China in NE Japan Evidenced by Detrital Zircon. *Gff* 136, 116–119. doi:10.1080/11035897.2014.893254

Jamieson, R. A., and Beaumont, C. (2013). On the Origin of Orogens. *Geol. Soc. Am. Bull.* 125, 1671–1702. doi:10.1130/b30855.1

Jiang, Y., Xing, G., Yuan, Q., Zhao, X., Duan, Z., and Dong, X. (2016). The First Discovery of Permian Metamorphic Rocks in Zhoushan Islands, Zhejiang Province. *Geol. Bull. China* 35, 1046–1055.

Kawabata, R., Imayama, T., Kato, T., Oh, C. W., Horie, K., and Takehara, M. (2021). Multi-stage Metamorphic History of the Oki Gneisses in Japan: Implications for Paleoproterozoic Metamorphism and Tectonic Correlations in Northeastern Asia. *J. Metamorph. Geol.* 40, 257–286. doi:10.1111/jmg.12627

Kimura, K., Hayasaka, Y., Shibata, T., Kawaguchi, K., and Fujiwara, H. (2019). Discovery of Paleoproterozoic 1.85 Ga Granitoid Bodies from the Maizuru Terrane in the Tsuwano Area, Shimane Prefecture, Southwest Japan and its Geologic Implications. *Jour. Geol. Soc. Jpn.* 125, 153–165. doi:10.5575/geosoc.2018.0050

Kwon, S., Sajeev, K., Mitra, G., Park, Y., Kim, S. W., and Ryu, I.-C. (2009). Evidence for Permo-Triassic Collision in Far East Asia: The Korean Collisional Orogen. *Earth Planet. Sci. Lett.* 279, 340–349. doi:10.1016/j.epsl.2009.01.016

Li, C.-f., Li, X.-h., Li, Q.-l., Guo, J.-h., and Li, X.-h. (2011a). Directly Determining 143Nd/144Nd Isotope Ratios Using Thermal Ionization Mass Spectrometry for Geological Samples without Separation of Sm-Nd. *J. Anal. At. Spectrom.* 26, 2012. doi:10.1039/c0ja00081g

Li, C.-F., Li, X.-H., Li, Q.-L., Guo, J.-H., Li, X.-H., and Liu, T. (2011b). An Evaluation of a Single-step Extraction Chromatography Separation Method for Sm-Nd Isotope Analysis of Micro-samples of Silicate Rocks by High-Sensitivity Thermal Ionization Mass Spectrometry. *Anal. Chim. Acta* 706, 297–304. doi:10.1016/j.aca.2011.08.036

Li, J., Dong, S., Zhang, Y., Zhao, G., Johnston, S. T., Cui, J., et al. (2016a). New Insights into Phanerozoic Tectonics of South China: Part 1, Polyphase Deformation in the Jiuling and Lianyunshan Domains of the Central Jiangnan Orogen. *J. Geophys. Res. Solid Earth* 121, 3048–3080. doi:10.1002/2015jb012778

Li, J., Zhang, Y., Zhao, G., Johnston, S. T., Dong, S., Koppers, A., et al. (2017a). New Insights into Phanerozoic Tectonics of South China: Early Paleozoic Sinistral and Triassic Dextral Transpression in the East Wuyishan and Chencai Domains, NE Cathaysia. *Tectonics* 36, 819–853. doi:10.1002/2016tc004461

Li, L., Lin, S., Xing, G., Davis, D. W., Jiang, Y., Davis, W. J. (2016b). Ca. 830 Ma Back-Arc Type Volcanic Rocks in the Eastern Part of the Jiangnan Orogen: Implications for the Neoproterozoic Tectonic Evolution of South China Block. *Precambrian Res.* 275, 209–224. doi:10.1016/j.precamres.2016.01.016

Li, S., Jahn, B.-m., Zhao, S., Dai, L., Li, X., Suo, Y., et al. (2017b). Triassic Southeastward Subduction of North China Block to South China Block: Insights from New Geological, Geophysical and Geochemical Data. *Earth-Science Rev.* 166, 270–285. doi:10.1016/j.earscirev.2017.01.009

Li, S., Santosh, M., Zhao, G., Zhang, G., and Jin, C. (2012a). Intracontinental Deformation in a Frontier of Super-convergence: A Perspective on the Tectonic Milieu of the South China Block. *J. Asian Earth Sci.* 49, 313–329. doi:10.1016/j.jseaes.2011.07.026

Li, S. Z., Li, X. Y., Shu-Juan, Y., Chao, L., Xin, G., Ling-Li, W., et al. (2016e). Global Early Paleozoic Orogens (III): Intracontinental Orogen in South China. *J. Jilin Univ. (Earth Sci. Ed.* 46, 1005–1025. doi:10.13278/j.cnki.jjuese.201604103

Li, S. Z., Yang, C., Zhao, S. J., Li, X. Y., Ling-Li, Y., Shan, L., et al. (2016d). Global Early Paleozoic Orogens (II): Collision-type Orogeny. *J. Jilin Univ. (Earth Sci. Ed.* 46, 946–967. doi:10.13278/j.cnki.jjuese.201604102

Li, S. Z., Yang, C., Zhao, S. J., Li, X. Y., Shu-Yan, G., Ling-Li, Y., et al. (2016c). Global Early Paleozoic Orogens (I): Subduction-accretionary-type Orogeny. *J. Jilin Univ. (Earth Sci. Ed.* 46, 968–1004. doi:10.13278/j.cnki.jjuese.201604101

Li, W., Li, X., and Li, Z. (2005). Neoproterozoic Bimodal Magmatism in the Cathaysia Block of South China and its Tectonic Significance. *Precambrian Res.* 136, 51–66. doi:10.1016/j.precamres.2004.09.008

Li, W., Ma, C., Liu, Y., and Robinson, P. T. (2012b). Discovery of the Indosinian Aluminum A-type Granite in Zhejiang Province and its Geological Significance. *Sci. China Earth Sci.* 55, 13–25. doi:10.1007/s11430-011-4351-6

Li, W. X., Li, X. H., and Li, Z. X. (2010a). Ca. 850 Ma Bimodal Volcanic Rocks in Northeastern Jiangxi Province, South China: Initial Extension during the Breakup of Rodinia? *Am. J. Sci.* 310, 951–980. doi:10.2475/09.2010.08

Li, X.-H., Li, W.-X., Li, Q.-L., Wang, X.-C., Liu, Y., and Yang, Y.-H. (2010b). Petrogenesis and Tectonic Significance of the ~850 Ma Gangbian Alkaline Complex in South China: Evidence from *In Situ* Zircon U-Pb Dating, Hf-O Isotopes and Whole-Rock Geochemistry. *Lithos* 114, 1–15. doi:10.1016/j.lithos.2009.07.011

Li, X.-H., Li, W.-X., Li, Z.-X., Lo, C.-H., Wang, J., Ye, M.-F., et al. (2009a). Amalgamation between the Yangtze and Cathaysia Blocks in South China: Constraints from SHRIMP U-Pb Zircon Ages, Geochemistry and Nd-Hf Isotopes of the Shuangxiwu Volcanic Rocks. *Precambrian Res.* 174, 117–128. doi:10.1016/j.precamres.2009.07.004

Li, X.-H., Li, Z.-X., and Li, W.-X. (2014). Detrital Zircon U-Pb Age and Hf Isotope Constrains on the Generation and Reworking of Precambrian Continental Crust in the Cathaysia Block, South China: A Synthesis. *Gondwana Res.* 25, 1202–1215. doi:10.1016/j.gr.2014.01.003

Li, X.-H., Liu, Y., Li, Q.-L., Guo, C.-H., and Chamberlain, K. R. (2009b). Precise Determination of Phanerozoic Zircon Pb/Pb Age by Multicollector SIMS without External Standardization. *Geochem. Geophys. Geosyst.* 10. doi:10.1029/2009GC002400

Li, X.-H., Long, W.-G., Li, Q.-L., Liu, Y., Zheng, Y.-F., Yang, Y.-H., et al. (2010c). Penglai Zircon Megacrysts: a Potential New Working Reference Material for Microbeam Determination of Hf-O Isotopes and U-Pb Age. *Geostand. Geoanalytical Res.* 34, 117–134. doi:10.1111/j.1751-908x.2010.00036.x

Li, X.-h. (1997). Timing of the Cathaysia Block Formation: Constraints from SHRIMP U-Pb Zircon Geochronology. *Episodes* 20, 188–192. doi:10.18814/epiiugs/1997/v20i3/008

Li, X. H., Li, Z. X., Li, W. X., and Wang, Y. (2006). Initiation of the Indosinian Orogeny in South China: Evidence for a Permian Magmatic Arc on Hainan Island. *J. Geol.* 114, 341–353. doi:10.1086/501222

Li, Z.-X., and Li, X.-H. (2007). Formation of the 1300-km-wide Intracontinental Orogen and Postorogenic Magmatic Province in Mesozoic South China: A Flat-Slab Subduction Model. *Geol* 35, 179–182. doi:10.1130/g23193a.1

Li, Z. X. (1998). "Tectonic History of the Major East Asian Lithospheric Blocks Since the Mid-Proterozoic—A Synthesis," in *Mantle Dynamics and Plate Interactions in East Asia*. Editor M. F. J. Flower, S.-L. Chung, C.-H. Lo, and T.-Y. Lee (Washington, DC: American Geophysical Unio), 221–243. doi:10.1029/GD027p0221

Lin, S., Xing, G., Davis, D. W., Yin, C., Wu, M., Li, L., et al. (2018). Appalachian-style Multi-Terrane Wilson Cycle Model for the Assembly of South China. *Geology* 46, 319–322. doi:10.1130/g39806.1

Lin, W., Wang, Q., and Chen, K. (2008). Phanerozoic Tectonics of South China Block: New Insights from the Polyphase Deformation in the Yunkai Massif. *Tectonics* 27, 1–16. doi:10.1029/2007tc002207

Liu, F. L., Gerdes, A., Liou, J. G., Xue, H. M., and Liang, F. H. (2006). SHRIMP U-Pb Zircon Dating from Sulu-Dabie Dolomitic Marble, Eastern China: Constraints on Prograde, Ultrahigh-Pressure and Retrograde Metamorphic Ages. *J. Metamorph. Geol.* 24, 569–589. doi:10.1111/j.1525-1314.2006.00655.x

Liu, F., Xu, Z., Liou, J. G., and Song, B. (2004). SHRIMP U-Pb Ages of Ultrahigh-Pressure and Retrograde Metamorphism of Gneisses, South-Western Sulu Terrane, Eastern China. *J. Metamorph. Geol.* 22, 315–326. doi:10.1111/j.1525-1314.2004.00516.x

Liu, L., Li, S., Dai, L., Suo, Y., Liu, B., Zhang, G., et al. (2012a). Geometry and Timing of Mesozoic Deformation in the Western Part of the Xuefeng Tectonic Belt, South China: Implications for Intra-continental Deformation. *J. Asian Earth Sci.* 49, 330–338. doi:10.1016/j.jseaes.2011.09.026

Liu, Q., Yu, J.-H., Wang, Q., Su, B., Zhou, M.-F., Xu, H., et al. (2012b). Ages and Geochemistry of Granites in the Pingtan-Dongshan Metamorphic Belt, Coastal South China: New Constraints on Late Mesozoic Magmatic Evolution. *Lithos* 150, 268–286. doi:10.1016/j.lithos.2012.06.031

Liu, X. (1993). High-P Metamorphic Belt in Central China and its Possible Eastward Extension to Korea. *J. Petrological Soc. Korea* 2, 9–18.

Lu, H. F. (2006). On the Cathaysian Oldland. *Geol. J. China Univ.* 12, 413–417.

Ludwig, K. (2012). *User's Manual for Isoplot Version 3.75–4.15: A Geochronological Toolkit for Microsoft Excel.* Berkley: Geochronological Center Special Publication.

Matsunaga, S., Tsujimori, T., Miyashita, A., Aoki, S., Aoki, K., Pastor-Galán, D., et al. (2021). Reappraisal of the Oldest High-Pressure Type Schist in Japan: New

Zircon U-Pb Age of the Kitomyo Schist of the Kurosegawa Belt. *Lithos*, 380–381. doi:10.1016/j.lithos.2020.105898

Middlemost, E. A. K. (1994). Naming Materials in the Magma/igneous Rock System. *Earth-Science Rev.* 37, 215–224. doi:10.1016/0012-8252(94)90029-9

Miyashiro, A. (1961). Evolution of Metamorphic Belts. *J. Petrology* 2, 277–311. doi:10.1093/petrology/2.3.277

Miyashiro, A. (1973). Paired and Unpaired Metamorphic Belts. *Tectonophysics* 17, 241–254. doi:10.1016/0040-1951(73)90005-x

O'Brien, P. J. (1993). Partially Retrograded Eclogites of the Münchberg Massif, Germany: Records of a Multi-Stage Variscan Uplift History in the Bohemian Massif. *J. Metamorph. Geol.* 11, 241–260. doi:10.1111/j.1525-1314.1993.tb00145.x

Oh, C. W., and Kim, Y. H. (2021). The Geological Correlation between the Korean Peninsula and China from Paleoproterozoic to Triassic and the Comparative Evaluation Among the Permo-Triassic Collision Models in the Northeast Asia. *jgsk* 57, 369–412. doi:10.14770/jgsk.2021.57.4.369

Okay, A. I., and Celal Şengör, A. M. (1992). Evidence for Intracontinental Thrust-Related Exhumation of the Ultra-high-pressure Rocks in China. *Geol* 20, 411–414. doi:10.1130/0091-7613(1992)020<0411:efitre>2.3.co;2

Pastor-Galán, D., Spencer, C. J., Furukawa, T., and Tsujimori, T. (2021). Evidence for Crustal Removal, Tectonic Erosion and Flare-Ups from the Japanese Evolving Forearc Sediment Provenance. *Earth Planet. Sci. Lett.* 564. doi:10.1016/j.epsl.2021.116893

Pearce, J. A. (1975). Basalt Geochemistry Used to Investigate Past Tectonic Environments on Cyprus. *Tectonophysics* 25, 41–67. doi:10.1016/0040-1951(75)90010-4

Raimondo, T., Hand, M., and Collins, W. J. (2014). Compressional Intracontinental Orogens: Ancient and Modern Perspectives. *Earth-Science Rev.* 130, 128–153. doi:10.1016/j.earscirev.2013.11.009

Ratschbacher, L., Hacker, B. R., Calvert, A., Webb, L. E., Grimmer, J. C., McWilliams, M. O., et al. (2003). Tectonics of the Qinling (Central China): Tectonostratigraphy, Geochronology, and Deformation History. *Tectonophysics* 366, 1–53. doi:10.1016/s0040-1951(03)00053-2

Ree, J.-H., Cho, M., Kwon, S.-T., and Nakamura, E. (1996). Possible Eastward Extension of Chinese Collision Belt in South Korea: the Imjingang Belt. *Geol* 24, 1071–1074. doi:10.1130/0091-7613(1996)024<1071:peeocc>2.3.co;2

Ren, J. S. (1984). The Indosinian Orogeny and its Significance in the Tectonic Evolution of China. *Bull. Chin. Acad. Geol. Sci.* 9, 31–44.

Rowley, D. B., Ziegler, A. M., Gyou, N., Hsü, K. J., Shu, S., Jiliang, L., et al. (1989). Comment and Reply on "Mesozoic Overthrust Tectonics in South China". *Geol* 17, 384–387. doi:10.1130/0091-7613(1989)017<0384:caromo>2.3.co;2

Sandiford, M., and Hand, M. (1998). Controls on the Locus of Intraplate Deformation in Central Australia. *Earth Planet. Sci. Lett.* 162, 97–110. doi:10.1016/s0012-821x(98)00159-9

Sandiford, M., Hand, M., and McLaren, S. (2001). Tectonic Feedback, Intraplate Orogeny and the Geochemical Structure of the Crust: a Central Australian Perspective. *Geol. Soc. Lond. Spec. Publ.* 184, 195–218. doi:10.1144/gsl.sp.2001.184.01.10

Shu, L.-S., Faure, M., Yu, J.-H., and Jahn, B.-M. (2011). Geochronological and Geochemical Features of the Cathaysia Block (South China): New Evidence for the Neoproterozoic Breakup of Rodinia. *Precambrian Res.* 187, 263–276. doi:10.1016/j.precamres.2011.03.003

Shu, L. (2012). An Analysis of Principal Features of Tectonic Evolution of South China Block. *Geol. Bull. China* 31, 1035–1053.

Shu, L., Deng, P., Yu, J., Wang, Y., and Jiang, S. (2008a). The Age and Tectonic Environment of the Rhyolitic Rocks on the Western Side of Wuyi Mountain, South China. *Sci. China Ser. D-Earth Sci.* 51, 1053–1063. doi:10.1007/s11430-008-0078-4

Shu, L., Faure, M., Wang, B., Zhou, X., and Song, B. (2008b). Late Palaeozoic-Early Mesozoic Geological Features of South China: Response to the Indosinian Collision Events in Southeast Asia. *Comptes Rendus Geosci.* 340, 151–165. doi:10.1016/j.crte.2007.10.010

Shu, L. S. (2006). Pre-Devonian Tectonic Evolution of South China: from Cathaysian Block to Caledonian Period Folded Orogenic Belt. *Geol. J. China Univ.* 12, 418–431.

Shu, L., Song, M., and Yao, J. (2018). Appalachian-style Multi-Terrane Wilson Cycle Model for the Assembly of South China: COMMENT. *Geology* 46, e445. doi:10.1130/g40213c.1

Shu, L., Wang, J., and Yao, J. (2019). Tectonic Evolution of the Eastern Jiangnan Region, South China: New Findings and Implications on the Assembly of the Rodinia Supercontinent. *Precambrian Res.* 322, 42–65. doi:10.1016/j.precamres.2018.12.007

Sláma, J., Košler, J., Condon, D. J., Crowley, J. L., Gerdes, A., Hanchar, J. M., et al. (2008). Plešovice Zircon—A New Natural Reference Material for U–Pb and Hf Isotopic Microanalysis. *Chem. Geol.* 249, 1–35. doi:10.1016/j.chemgeo.2007.11.005

Söderlund, U., Patchett, P. J., Vervoort, J. D., and Isachsen, C. E. (2004). The 176Lu Decay Constant Determined by Lu–Hf and U–Pb Isotope Systematics of Precambrian Mafic Intrusions. *Earth Planet. Sci. Lett.* 219, 311–324. doi:10.1016/S0012-821X(04)00012-3

Sokoutis, D., and Willingshofer, E. (2011). Decoupling during Continental Collision and Intra-plate Deformation. *Earth Planet. Sci. Lett.* 305, 435–444. doi:10.1016/j.epsl.2011.03.028

Stacey, J. S., and Kramers, J. D. (1975). Approximation of Terrestrial Lead Isotope Evolution by a Two-Stage Model. *Earth Planet. Sci. Lett.* 26, 207–221. doi:10.1016/0012-821x(75)90088-6

Sun, L.-Q., Ling, H.-F., Shen, W.-Z., Wang, K.-X., and Huang, G.-L. (2017). Petrogenesis of Two Triassic A-type Intrusions in the Interior of South China and Their Implications for Tectonic Transition. *Lithos* 284, 642–653. doi:10.1016/j.lithos.2017.05.006

Sun, S.-S., and McDonough, W. F. (1989). Chemical and Isotopic Systematics of Oceanic Basalts: Implications for Mantle Composition and Processes. *Geol. Soc. Lond. Spec. Publ.* 42, 313–345. doi:10.1144/gsl.sp.1989.042.01.19

Sun, Y., Ma, C., Liu, Y., and She, Z. (2011). Geochronological and Geochemical Constraints on the Petrogenesis of Late Triassic Aluminous A-type Granites in Southeast China. *J. Asian Earth Sci.* 42, 1117–1131. doi:10.1016/j.jseaes.2011.06.007

Taira, A. (2001). Tectonic Evolution of the Japanese Island Arc System. *Annu. Rev. Earth Planet. Sci.* 29, 109–134. doi:10.1146/annurev.earth.29.1.109

Takahashi, Y., Cho, D.-L., Mao, J., Zhao, X., and Yi, K. (2018). SHRIMP U-Pb Zircon Ages of the Hida Metamorphic and Plutonic Rocks, Japan: Implications for Late Paleozoic to Mesozoic Tectonics Around the Korean Peninsula. *Isl. Arc* 27. doi:10.1111/iar.12220

Tatsumi, Y., Kani, T., Ishizuka, H., Maruyama, S., and Nishimura, Y. (2000). Activation of Pacific Mantle Plumes during the Carboniferous: Evidence from Accretionary Complexes in Southwest Japan. *Geology* 28, 580–582. doi:10.1130/0091-7613(2000)028<0580:aopmpd>2.3.co;2

Tsujimori, T., Liou, J. G., Ernst, W. G., and Itaya, T. (2006). Triassic Paragonite- and Garnet-Bearing Epidote-Amphibolite from the Hida Mountains, Japan. *Gondwana Res.* 9, 167–175. doi:10.1016/j.gr.2005.03.001

Tsujimori, T., and Liou, J. G. (2004). Metamorphic Evolution of Kyanite-Staurolite-Bearing Epidote-Amphibolite from the Early Palaeozoic Oeyama Belt, SW Japan. *J. Metamorph. Geol.* 22, 301–313. doi:10.1111/j.1525-1314.2004.00515.x

Tsujimori, T. (2002). Prograde and Retrograde P-T Paths of the Late Paleozoic Glaucophane Eclogite from the Renge Metamorphic Belt, Hida Mountains, Southwestern Japan. *Int. Geol. Rev.* 44, 797–818. doi:10.2747/0020-6814.44.9.797

Tsutsumi, Y., Isozaki, Y., and Terabayashi, M. (2017). The Most Continent-Sided Occurrence of the Phanerozoic Subduction-Related Orogens in SW Japan: Zircon U-Pb Dating of the Mizoguchi Gneiss on the Western Foothill of Mt. Daisen Volcano in Tottori. *J. Asian Earth Sci.* 145, 530–541. doi:10.1016/j.jseaes.2017.06.028

Valley, J. W., Chiarenzelli, J. R., and McLelland, J. M. (1994). Oxygen Isotope Geochemistry of Zircon. *Earth Planet. Sci. Lett.* 126, 187–206. doi:10.1016/0012-821x(94)90106-6

Vavra, G. (1990). On the Kinematics of Zircon Growth and its Petrogenetic Significance: a Cathodoluminescence Study. *Contr. Mineral. Pet.* 106, 90–99. doi:10.1007/bf00306410

Wakita, K. (2013). Geology and Tectonics of Japanese Islands: A Review - the Key to Understanding the Geology of Asia. *J. Asian Earth Sci.* 72, 75–87. doi:10.1016/j.jseaes.2012.04.014

Wallis, S. R., Yamaoka, K., Mori, H., Ishiwatari, A., Miyazaki, K., and Ueda, H. (2020). The Basement Geology of Japan from A to Z. *Isl. Arc* 29, e12339. doi:10.1111/iar.12339

Wan, Y., Liu, D., Wilde, S. A., Cao, J., Chen, B., Dong, C., et al. (2010). Evolution of the Yunkai Terrane, South China: Evidence from SHRIMP Zircon U-Pb Dating, Geochemistry and Nd Isotope. *J. Asian Earth Sci.* 37, 140–153. doi:10.1016/j.jseaes.2009.08.002

Wang, J. G., Yu, S. Q., Zhao, X. D., Wu, M., Gu, G. M., and Hu, Y. H. (2014c). The Discovery of Paleoproterozoic Mafic-Ultramafic Rocks in the Wuyishan Block: Description of Profile and Characteristics of Petrology, Petrography and Isotope Geochronology. *Acta Petrologica Mineralogica* 33, 617–629.

Wang, J., and Li, Z. (2003). History of Neoproterozoic Rift Basins in South China: Implications for Rodinia Break-Up. *Precambrian Res.* 122, 141–158. doi:10.1016/s0301-9268(02)00209-7

Wang, Q., Li, J.-W., Jian, P., Zhao, Z.-H., Xiong, X.-L., Bao, Z.-W., et al. (2005a). Alkaline Syenites in Eastern Cathaysia (South China): Link to Permian-Triassic Transtension. *Earth Planet. Sci. Lett.* 230, 339–354. doi:10.1016/j.epsl.2004.11.023

Wang, X.-C., Li, X.-H., Li, W.-X., and Li, Z.-X. (2007). Ca. 825 Ma Komatiitic Basalts in South China: First Evidence for >1500 °C Mantle Melts by a Rodinian Mantle Plume. *Geol* 35, 1103. doi:10.1130/g23878a.1

Wang, X.-C., Li, X.-h., Li, Z.-X., Li, Q.-l., Tang, G.-Q., Gao, Y.-Y., et al. (2012a). Episodic Precambrian Crust Growth: Evidence from U-Pb Ages and Hf-O Isotopes of Zircon in the Nanhua Basin, Central South China. *Precambrian Res.* 222, 386–403. doi:10.1016/j.precamres.2011.06.001

Wang, X.-L., Shu, L.-S., Xing, G.-F., Zhou, J.-C., Tang, M., Shu, X.-J., et al. (2012b). Post-orogenic Extension in the Eastern Part of the Jiangnan Orogen: Evidence from Ca 800-760Ma Volcanic Rocks. *Precambrian Res.* 222, 404–423. doi:10.1016/j.precamres.2011.07.003

Wang, X.-L., Zhou, J.-C., Griffin, W. L., Zhao, G., Yu, J.-H., Qiu, J.-S., et al. (2014a). Geochemical Zonation across a Neoproterozoic Orogenic Belt: Isotopic Evidence from Granitoids and Metasedimentary Rocks of the Jiangnan Orogen, China. *Precambrian Res.* 242, 154–171. doi:10.1016/j.precamres.2013.12.023

Wang, X., Liou, J. G., and Mao, H. K. (1989). Coesite-bearing Eclogite from the Dabie Mountains in Central China. *Geol* 17, 1085–1088. doi:10.1130/0091-7613(1989)017<1085:cbeftd>2.3.co;2

Wang, Y., Fan, W., Zhang, G., and Zhang, Y. (2013a). Phanerozoic Tectonics of the South China Block: Key Observations and Controversies. *Gondwana Res.* 23, 1273–1305. doi:10.1016/j.gr.2012.02.019

Wang, Y., Wang, Y., Zhang, Y., Cawood, P. A., Qian, X., Gan, C., et al. (2021). Triassic Two-Stage Intra-continental Orogensis of the South China Block, Driven by Paleotethyan Closure and Interactions with Adjoining Blocks. *J. Asian Earth Sci.* 206. doi:10.1016/j.jseaes.2020.104648

Wang, Y., Wu, C., Zhang, A., Fan, W., Zhang, Y., Zhang, Y., et al. (2012c). Kwangsian and Indosinian Reworking of the Eastern South China Block: Constraints on Zircon U-Pb Geochronology and Metamorphism of Amphibolites and Granulites. *Lithos* 150, 227–242. doi:10.1016/j.lithos.2012.04.022

Wang, Y., Zhang, A., Cawood, P. A., Fan, W., Xu, J., Zhang, G., et al. (2013b). Geochronological, Geochemical and Nd-Hf-Os Isotopic Fingerprinting of an Early Neoproterozoic Arc-Back-Arc System in South China and its Accretionary Assembly along the Margin of Rodinia. *Precambrian Res.* 231, 343–371. doi:10.1016/j.precamres.2013.03.020

Wang, Y., Zhang, A., Fan, W., Geng, H., Zou, H., and Bi, X. (2014b). Early Neoproterozoic Accretionary Assemblage in the Cathaysia Block: Geochronological, Lu-Hf Isotopic and Geochemical Evidence from Granitoid Gneisses. *Precambrian Res.* 249, 144–161. doi:10.1016/j.precamres.2014.05.003

Wang, Y., Zhang, Y., Fan, W., and Peng, T. (2005b). Structural Signatures and 40Ar/39Ar Geochronology of the Indosinian Xuefengshan Tectonic Belt, South China Block. *J. Struct. Geol.* 27, 985–998. doi:10.1016/j.jsg.2005.04.004

Winchester, J. A., and Floyd, P. A. (1977). Geochemical Discrimination of Different Magma Series and Their Differentiation Products Using Immobile Elements. *Chem. Geol.* 20, 325–343. doi:10.1016/0009-2541(77)90057-2

Wood, D. A. (1980). The Application of a ThHfTa Diagram to Problems of Tectonomagmatic Classification and to Establishing the Nature of Crustal Contamination of Basaltic Lavas of the British Tertiary Volcanic Province. *Earth Planet. Sci. Lett.* 50, 11–30. doi:10.1016/0012-821x(80)90116-8

Woodhead, J. D., and Hergt, J. M. (2005). A Preliminary Appraisal of Seven Natural Zircon Reference Materials for In Situ Hf Isotope Determination. Geostand. Geoanalyt Res. 29, 183–195. doi:10.1111/j.1751-908x.2005.tb00891.x

Wu, F.-Y., Yang, Y.-H., Xie, L.-W., Yang, J.-H., and Xu, P. (2006). Hf Isotopic Compositions of the Standard Zircons and Baddeleyites Used in U-Pb Geochronology. Chem. Geol. 234, 105–126. doi:10.1016/j.chemgeo.2006.05.003

Wu, Y.-B., and Zheng, Y.-F. (2013). Tectonic Evolution of a Composite Collision Orogen: An Overview on the Qinling-Tongbai-Hong'an-Dabie-Sulu Orogenic Belt in Central China. Gondwana Res. 23, 1402–1428. doi:10.1016/j.gr.2012.09.007

Xia, Y., Xu, X.-S., and Zhu, K.-Y. (2012). Paleoproterozoic S- and A-type Granites in Southwestern Zhejiang: Magmatism, Metamorphism and Implications for the Crustal Evolution of the Cathaysia Basement. Precambrian Res. 216, 177–207. doi:10.1016/j.precamres.2012.07.001

Xia, Y., Yin, C., Lin, S., Zhang, J., Qian, J., Wu, S., et al. (2021). Metamorphism and Geochronology of High-Pressure Mafic Granulites (Retrograded Eclogites?) in East Cathaysia Terrane of South China: Implications for Mesozoic Tectonic Evolution. GSA Bull. 134, 832. doi:10.1130/B36025.1

Xiang, H., Zhang, L., Zhou, H., Zhong, Z., Zeng, W., Liu, R., et al. (2008). U-pb Zircon Geochronology and Hf Isotope Study of Metamorphosed Basic-Ultrabasic Rocks from Metamorphic Basement in Southwestern Zhejiang: The Response of the Cathaysia Block to Indosinian Orogenic Event. Sci. China Ser. D-Earth Sci. 51, 788–800. doi:10.1007/s11430-008-0053-0

Xie, L., Zhang, Y., Zhang, H., Sun, J., and Wu, F. (2008). In Situ simultaneous Determination of Trace Elements, U-Pb and Lu-Hf Isotopes in Zircon and Baddeleyite. Sci. Bull. 53, 1565–1573. doi:10.1007/s11434-008-0086-y

Xing, G. F., Li, L. M., Jiang, Y., Feng, Y. F., Lu, Q. D., Chen, Z. H., et al. (2014). Petrogenetic Process of Cretaceous 'gneissic' Magma-Mixed Complex in the Changle-Nan'ao Structure Zone, Fujian Province: a Case Study on Xiaocuo Intrusion. Resour. Surgey Environ. 35, 79–94.

Xing, G., Lu, Q., Jiang, Y., Nie, T., Chen, R., Feng, Y., et al. (2010). Identification and Significance of "gneissic" Magma-Mixed Complex in the Changle-Nan'ao Fault Zone, Southeastern Fujian, Chian. Geol. Bull. China 29, 31–43.

Xu, S., Ai, O., Ji, S., Amc, S., Su, W., Liu, Y., et al. (1992). Diamond from the Dabie Shan Metamorphic Rocks and its Implication for Tectonic Setting. Science 256, 80–82.

Xu, X., O'Reilly, S. Y., Griffin, W. L., Wang, X., Pearson, N. J., and He, Z. (2007). The Crust of Cathaysia: Age, Assembly and Reworking of Two Terranes. Precambrian Res. 158, 51–78. doi:10.1016/j.precamres.2007.04.010

Yang, Y.-h., Zhang, H.-f., Chu, Z.-y., Xie, L.-w., and Wu, F.-y. (2010). Combined Chemical Separation of Lu, Hf, Rb, Sr, Sm and Nd from a Single Rock Digest and Precise and Accurate Isotope Determinations of Lu-Hf, Rb-Sr and Sm-Nd Isotope Systems Using Multi-Collector ICP-MS and TIMS. Int. J. Mass Spectrom. 290, 120–126. doi:10.1016/j.ijms.2009.12.011

Yang, Z.-Y., and Jiang, S.-Y. (2019). Detrital Zircons in Metasedimentary Rocks of Mayuan and Mamianshan Group from Cathaysia Block in Northwestern Fujian Province, South China: New Constraints on Their Formation Ages and Paleogeographic Implication. Precambrian Res. 320, 13–30. doi:10.1016/j.precamres.2018.10.004

Yao, J., Shu, L., Santosh, M., and Zhao, G. (2014). Neoproterozoic Arc-Related Mafic-Ultramafic Rocks and Syn-Collision Granite from the Western Segment of the Jiangnan Orogen, South China: Constraints on the Neoproterozoic Assembly of the Yangtze and Cathaysia Blocks. Precambrian Res. 243, 39–62. doi:10.1016/j.precamres.2013.12.027

Yin, A., Nie, S., Craig, P., Harrison, T. M., Ryerson, F. J., Xianglin, Q., et al. (1998). Late Cenozoic Tectonic Evolution of the Southern Chinese Tian Shan. Tectonics 17, 1–27. doi:10.1029/97tc03140

Yin, H. F., Wu, S. B., Du, Y. S., and Peng, Y. Q. (1999). South China Defined as Part of Tethyan Archipelagic Ocean System. J. China Univ. Geosciences- Earth Sci. 24, 3–14.

Yu, J.-H., O'Reilly, S. Y., Wang, L., Griffin, W. L., Zhang, M., Wang, R., et al. (2008). Where Was South China in the Rodinia Supercontinent? Precambrian Res. 164, 1–15. doi:10.1016/j.precamres.2008.03.002

Yu, J.-H., O'Reilly, S. Y., Wang, L., Griffin, W. L., Zhou, M.-F., Zhang, M., et al. (2010). Components and Episodic Growth of Precambrian Crust in the Cathaysia Block, South China: Evidence from U-Pb Ages and Hf Isotopes of Zircons in Neoproterozoic Sediments. Precambrian Res. 181, 97–114. doi:10.1016/j.precamres.2010.05.016

Yu, J.-H., O'Reilly, S. Y., Zhou, M.-F., Griffin, W. L., and Wang, L. (2012). U-pb Geochronology and Hf-Nd Isotopic Geochemistry of the Badu Complex, Southeastern China: Implications for the Precambrian Crustal Evolution and Paleogeography of the Cathaysia Block. Precambrian Res. 222, 424–449. doi:10.1016/j.precamres.2011.07.014

Yu, J.-H., Wang, L., O'Reilly, S. Y., Griffin, W. L., Zhang, M., Li, C., et al. (2009). A Paleoproterozoic Orogeny Recorded in a Long-Lived Cratonic Remnant (Wuyishan Terrane), Eastern Cathaysia Block, China. Precambrian Res. 174, 347–363. doi:10.1016/j.precamres.2009.08.009

Yu, J. H., Wei, Z. Y., Wang, L. J., and Sun, T. (2006). Cathaysia Block: a Young Continent Composed of Ancient Materials. Geol. J. China Univ. 04, 440–447.

Yu, J., O'Reilly, Y. S., Wang, L., Griffin, W. L., Jiang, S., Wang, R., et al. (2007). Finding of Ancient Materials in Cathaysia and Implication for the Formation of Precambrian Crust. Chin. Sci. Bull. 52, 13–22. doi:10.1007/s11434-007-0008-4

Yu, J., Zhou, X., O'Reilly, Y., Zhao, L., Griffin, W., Wang, R., et al. (2005). Formation History and Protolith Characteristics of Granulite Facies Metamorphic Rock in Central Cathaysia Deduced from U-Pb and Lu-Hf Isotopic Studies of Single Zircon Grains. Chin. Sci. Bull. 50, 2080–2089. doi:10.1360/982004-808

Yu, J., Zhou, X., Zhao, L., and Chen, X. (2003). Discovery and Implications of Granulite Facies Metamorphic Rocks in the Eastern Nanling, China. Acta Petrol. Sin. 19, 461–467.

Zeh, A., Gerdes, A., Klemd, R., and Barton, J. M. (2007). Archaean to Proterozoic Crustal Evolution in the Central Zone of the Limpopo Belt (South Africa-Botswana): Constraints from Combined U-Pb and Lu-Hf Isotope Analyses of Zircon. J. Petrology 48, 1605–1639. doi:10.1093/petrology/egm032

Zeng, W., Zhang, L., Zhou, H., Zhong, Z., Xiang, H., Liu, R., et al. (2008). Caledonian Reworking of Paleoproterozoic Basement in the Cathaysia Block: Constraints from Zircon U-Pb Dating, Hf Isotopes and Trace Elements. Sci. Bull. 53, 895–904. doi:10.1007/s11434-008-0076-0

Zhai, M., Cong, B., Zhao, Z., Wang, Q., Wang, G., and Jiang, L. (1995). Petrological-tectonic Units in the Coesite-Bearing Metamorphic Terrain of the Dabie Mountains, Central China and Their Geotectonic Implications. J. Southeast Asian Earth Sci. 11, 1–13.

Zhai, M. G. (2009). Two Kinds of Granulites (HT-HP and HT-UHT) in North China Craton: Their Genetic Relation and Geotectonic Implications. Acta Petrol. Sin. 25, 1753–1771.

Zhai, M., Zhang, Y., Zhang, X., Wu, F., Peng, P., Li, Q., et al. (2016). Renewed Profile of the Mesozoic Magmatism in Korean Peninsula: Regional Correlation and Broader Implication for Cratonic Destruction in the North China Craton. Sci. China Earth Sci. 59, 2355–2388. doi:10.1007/s11430-016-0107-0

Zhang, G., Guo, A., Wang, Y., Li, S., Dong, Y., Liu, S., et al. (2013). Tectonics of South China Continent and its Implications. Sci. China Earth Sci. 56, 1804–1828. doi:10.1007/s11430-013-4679-1

Zhao, C., He, K., Mo, X., Tai, D., Ye, D., Ye, N., et al. (1996). Discovery and its Significance of Late Paleozoic Radiolarian Silicalite in Ophiolitic Melange of Northeastern Jiangxi Deep Fault Belt. Chin. Sci. Bull. 41, 667–670.

Zhao, G., Wang, Y., Huang, B., Dong, Y., Li, S., Zhang, G., et al. (2018a). Geological Reconstructions of the East Asian Blocks: From the Breakup of Rodinia to the Assembly of Pangea. Earth-Science Rev. 186, 262–286. doi:10.1016/j.earscirev.2018.10.003

Zhao, J.-H., Zhang, S.-B., and Wang, X.-L. (2018b). Neoproterozoic Geology and Reconstruction of South China. Precambrian Res. 309, 1–5. doi:10.1016/j.precamres.2018.02.004

Zhao, L., Cui, X., Zhai, M., Zhou, X., and Liu, B. (2019). Emplacement and Metamorphism of the Mafic Rocks from the Chencai Terrane within the Cathaysia Block: Implications for the Paleozoic Orogenesis of the South China Block. J. Asian Earth Sci. 173, 11–28. doi:10.1016/j.jseaes.2019.01.019

Zhao, L., Zhai, M., Santosh, M., and Zhou, X. (2017a). Early Mesozoic Retrograded Eclogite and Mafic Granulite from the Badu Complex of the Cathaysia Block, South China: Petrology and Tectonic Implications. Gondwana Res. 42, 84–103. doi:10.1016/j.gr.2016.10.002

Zhao, L., Zhai, M., Zhou, X., Santosh, M., and Ma, X. (2016). Thermal Gradient and Geochronology of a Paleozoic High-Grade Terrane in the Northeastern Cathaysia Block, South China. Tectonophysics 691, 311–327. doi:10.1016/j.tecto.2016.10.024

Zhao, L., Zhang, R.-c., Zhai, M.-G., and Zhou, X.-W. (2020). Major Lithologies of the High-Grade Zhoutan Terrane within the Cathaysia Block and Their

Tectonic Implications for the Neoproterozoic - Paleozoic South China. *Lithos* 372, 105664. doi:10.1016/j.lithos.2020.105664

Zhao, L., Zhou, X., Zhai, M., Liu, B., and Cui, X. (2018c). Petrologic and Zircon U-Pb Geochronological Characteristics of the Pelitic Granulites from the Badu Complex of the Cathaysia Block, South China. *J. Asian Earth Sci.* 158, 65–79. doi:10.1016/j.jseaes.2018.02.017

Zhao, L., Zhou, X., Zhai, M., Santosh, M., and Geng, Y. (2015). Zircon U-Th-Pb-Hf Isotopes of the Basement Rocks in Northeastern Cathaysia Block, South China: Implications for Phanerozoic Multiple Metamorphic Reworking of a Paleoproterozoic Terrane. *Gondwana Res.* 28, 246–261. doi:10.1016/j.gr.2014.03.019

Zhao, L., Zhou, X., Zhai, M., Santosh, M., Ma, X., Shan, H., et al. (2014). Paleoproterozoic Tectonic Transition from Collision to Extension in the Eastern Cathaysia Block, South China: Evidence from Geochemistry, Zircon U-Pb Geochronology and Nd-Hf Isotopes of a Granite-Charnockite Suite in Southwestern Zhejiang. *Lithos* 184, 259–280. doi:10.1016/j.lithos.2013.11.005

Zhao, Z.-F., Zheng, Y.-F., Chen, Y.-X., and Sun, G.-C. (2017b). Partial Melting of Subducted Continental Crust: Geochemical Evidence from Synexhumation Granite in the Sulu Orogen. *GSA Bull.* 129, 11. doi:10.1130/B31675.31671

Zhejiang, B. G. M. R. (1980). *Map Report of 1:2,000,000 Geological Map of Shengsi, Yuyao, Dinghai, Ningbo and Shenjiamen*, 7–15.

Zhou, X. M., and Li, W. X. (2000). Origin of Late Mesozoic Igneous Rocks in Southeastern China: Implications for Lithosphere Subduction and Underplating of Mafic Magmas. *Tectonophysics* 326, 269–287. doi:10.1016/s0040-1951(00)00120-7

Zhou, X., Sun, T., Shen, W., Shu, L., and Niu, Y. (2006). Petrogenesis of Mesozoic Granitoids and Volcanic Rocks in South China: a Response to Tectonic Evolution. *Episodes* 29, 26–33. doi:10.18814/epiiugs/2006/v29i1/004